Microchimica Acta (2024) 191:535
https://doi.org/10.1007/s00604-024-06592-x

REVIEW

Red and near-infrared light-activated photoelectrochemical nanobiosensors for biomedical target detection

Yeison Monsalve[1] · Andrés F. Cruz-Pacheco[1] · Jahir Orozco[1]

Received: 21 June 2024 / Accepted: 28 July 2024

Abstract
Photoelectrochemical (PEC) nanobiosensors integrate molecular (bio)recognition elements with semiconductor/plasmonic photoactive nanomaterials to produce measurable signals after light-induced reactions. Recent advancements in PEC nanobiosensors, using light-matter interactions, have significantly improved sensitivity, specificity, and signal-to-noise ratio in detecting (bio)analytes. Tunable nanomaterials activated by a wide spectral radiation window coupled to electrochemical transduction platforms have further improved detection by stabilizing and amplifying electrical signals. This work reviews PEC biosensors based on nanomaterials like metal oxides, carbon nitrides, quantum dots, and transition metal chalcogenides (TMCs), showing their superior optoelectronic properties and analytical performance for the detection of clinically relevant biomarkers. Furthermore, it highlights the innovative role of red light and NIR-activated PEC nanobiosensors in enhancing charge transfer processes, protecting them from biomolecule photodamage in vitro and in vivo applications. Overall, advances in PEC detection systems have the potential to revolutionize rapid and accurate measurements in clinical diagnostic applications. Their integration into miniaturized devices also supports the development of portable, easy-to-use diagnostic tools, facilitating point-of-care (POC) testing solutions and real-time monitoring.

Keywords Photoelectrochemical nanobiosensor · Photoactive nanomaterial · Red light · Near-infrared (NIR) · Analytical performance

Introduction

PEC nanobiosensors use nanoscale components and light-matter interaction to provide specific quantitative or semi-quantitative analytical information about a (bio)analyte. They convert biological signals into electrical signals under the influence of light. PEC nanobiosensors consist of nanostructured components linked to a molecular recognition element or bioreceptor that specifically binds to the analyte and a transducer that converts this interaction into a measurable electrical signal [1, 2]. Rather than referring to the nanometric size of the entire device, the term nanobiosensor in this review refers to a system with at least one nanostructure within its components [3], whose enhanced properties from the nanoscale dimension give place to new, improved features and functionalities when assembled into biosensing devices [4]. PEC nanobiosensors utilize the interaction of light with photoactive materials to follow electrochemical reactions, benefiting from enhanced charge separation and signal amplification [5]. They typically integrate molecular recognition elements and/or (bio)receptors (e.g., enzymes, antibodies, nanobodies, peptides, cellular receptors, nucleic acids, glycans, aptamers, among others) with photoactive nanomaterials (e.g., semiconductor and plasmonic materials) [6–9]. Characterized by their high sensitivity and specificity, PEC nanobiosensors offer significant advantages such as signal amplification, minimal background noise, and reduced photodamage. These sensors feature tunable optical properties, photostability, durability, and amenability for surface functionalization. By leveraging PEC approaches, these biosensors provide rapid response times, versatility, and multi-functionality [10]. The current or voltage response under irradiation with light of different wavelengths in PEC biosensors changes when a recognition event occurs on the transducer surface or electrode [11]. It allows for highly

✉ Jahir Orozco
grupo.tandemnanobioe@udea.edu.co

[1] Max Planck Tandem Group in Nanobioengineering, Institute of Chemistry, Faculty of Natural and Exact Sciences, University of Antioquia, Complejo Ruta N, Calle 67 No. 52-20, 050010 Medellín, Colombia

Published online: 14 August 2024

specific and sensitive detection of various analytes, making PEC biosensors a promising tool for diverse applications in medical diagnostics [12]. Additionally, PEC nanobiosensors can be manufactured rapidly and cost-effectively for single-use devices, enabling efficient measurement collection using disposable electrodes, simplifying sensor handling, reducing contamination risks, and eliminating laborious cleaning or maintenance steps [13]. This combination of high sensitivity, miniaturization, and disposable amenability makes PEC biosensors well-suited for rapid, cost-effective, and user-friendly bioanalytical applications [14].

Incorporating high-surface-area photostimulable nanomaterials onto transducer platforms has further enhanced the performance of PEC sensing devices [15]. These nanomaterials can improve energy transfer processes, amplifying transduction signals to achieve highly sensitive, stable, and reproducible devices [16]. In particular, plasmonic nanoparticles, such as noble metals like gold (Au) and silver (Ag), exhibit collective oscillations of free electrons on their surface. This phenomenon leads to the absorption, scattering, and amplification of electromagnetic signals in the visible and NIR regions of the spectrum [17]. Utilizing this spectral radiation range to stimulate plasmonic nanoparticles in PEC biosensing is advantageous, as it minimizes potential photodamage to biomolecules compared to ultraviolet (UV) radiation [18, 19]. By harnessing these advancements, plasmon nanoparticle-based PEC biosensors offer improved stability and analytical performance without compromising biointerface integrity, thereby facilitating sensitive analyte detection [20]. In PEC detection, light is crucial in exciting the photoactive species, generating an electrical signal for transduction, and facilitating the detection process [21]. Separating the excitation source from the detection system endows this technique with potentially higher sensitivity. This heightened sensitivity is specifically due to the ability to automate the system's excitation source, allowing it to be turned on and off in a specific time window. This automation enables a precise response to the detection of the analyte of interest, effectively eliminating background noise from secondary reactions that do not correspond to the PEC detection event of the system [22, 23]. Moreover, the ease of miniaturizing PEC biosensing systems renders them more effective than conventional optical and electrochemical methods [24, 25]. This efficacy is due to the favorable photogenerated charge transfer reactions at the modified electrode surface [26]. When the analyte is present in the sample, the resultant specific recognition events can directly or indirectly induce alterations in the PEC signal, used to monitor the analyte levels [27, 28].

The selection of the photoactive material stands out as one of the most critical steps in determining the analytical performance of PEC devices. This choice is vital for enhancing charge conversion at the photoactive surfaces [1]. In recent years, semiconductor nanomaterials have emerged as the most utilized photoactive materials for PEC biosensing applications [29]. Various factors influence the performance of PEC devices, including changes in the photon conversion properties of typical semiconductor materials employed in transducer platforms. These factors encompass temperature fluctuations, external light exposure, electric and magnetic fields, and alterations in their electronic states of valence and conduction bands [30–33]. Such changes result in a sensitive response and impart unique properties in photoelectricity, photoluminescence, electroluminescence, electrochemiluminescence, and thermoelectric phenomena [34–38]. Semiconductor nanostructures exhibit a robust absorption capacity and an inherent electronic band structure [39]. Innovations in semiconductor morphology, structure, or elemental composition can bolster charge transport, facilitating high photoelectric conversion efficiency [40, 41].

Even though plenty of reviews have already been reported in the literature [42–45], there is still a knowledge gap intended to fill in this topic. This work reviews the crucial role of PEC nanobiosensors in detecting a wide spectral range of bioanalytes, discussing their impact on analytical performance. It compares PEC detection approaches stimulated by the spectrum's red light and NIR regions and thoroughly outlines the technical characteristics of these PEC assays, including their physicochemical properties, signal sources, sensing formats, and signaling strategies. Additionally, it explores various photoactive nanomaterials currently employed in PEC applications, examining their compositional and structural properties to enhance biosensing methodologies for various bio-analyte detection scenarios. Finally, it showcases the potential of red light and NIR region sources to improve PEC performance and finalizes with concluding remarks and perspectives to better exploit transduction mode PEC-based devices.

Technical characteristics of photoelectrochemical biosensors

PEC explores the interaction between light and photoactive materials, resulting in the interconversion of photoelectric and chemical energy [46]. The physical interaction between the photoactive material and the electrode promotes the charge transfer generated by the photons absorbed from the material, producing electrons and holes. Sacrificial reagents or redox mediators in solution transfer electrons to the photogenerated holes to restrict charge recombination in the material. The charge transfer on the electrode is reflected in an increase in current or potential resulting from excitation with light [47]. PEC biosensors integrate photoactive materials and molecular biorecognition elements (bioreceptors) coupled to the electrode interface to detect various (bio)analytes [48]. The change of the PEC signal when the electrode

is exposed to defined spectral ranges of light irradiation evidences the biorecognition event between the bioreceptor and the target (bio)analyte.

Conventional photodetection systems encompass four key components, as illustrated in Fig. 1. First is the excitation source (light source), followed by the signal transduction platform, which consists of the electrode, photoactive material, and molecular recognition elements. The third component is related to the redox mediator dissolved in an electrolytic medium. Finally, the PEC signal-reading system [49]. Multiple interconnected physical and chemical processes are essential to generate the signal. Initially, photons are absorbed, initiating a charge separation process in the material. Subsequently, charges migrate and recombine at the interface between the photoactive material on the working electrode and the redox mediator [50].

Efficiently converting photons into electric charge is a crucial factor in PEC processes [51, 52]. PEC devices integrate light as an excitation source to generate an increased electrical signal, improving sensitivity compared to conventional electrochemical processes [53, 54].

Photoactive nanomaterials

A photoactive nanomaterial can generate chemical or physical changes when interacting with electromagnetic radiation, usually in detection systems in the ultraviolet–visible (UV–vis) and NIR regions [55, 56]. The functionality of a photoactive material involves the absorption of light energy, the generation of electron–hole pairs, and a specific response that depends on its structural properties and the surrounding medium [57]. Integrating nanostructured materials into PEC biosensors offers advantages, including increased surface area, improved PEC features, bioconjugation, enhanced analytical properties, and the potential for miniaturization and amenability for portable sensing devices [58]. The light-sensitive nanostructured material interacts closely with the electrode and facilitates the transduction of the biochemical interaction into a quantifiable electrochemical signal [59]. The choice of a photoactive nanomaterial depends on the requirements of the PEC sensing application, encompassing the target analyte, detection sensitivity, and operating conditions [60]. Consequently, research on new photoactive materials would reinforce the versatility and functionality of PEC detection in bioanalysis applications [61, 62].

Physicochemical considerations

Specific physicochemical parameters play a pivotal role in comprehending the performance of photoactive nanomaterials [63]. To effectively absorb electromagnetic radiation and generate charge carriers leading to PEC detection, these materials must initially possess optical properties, including energy absorption and emission, as well as high quantum yield and extinction coefficient [64]. The morphology, atomic configurations, and nanostructure's

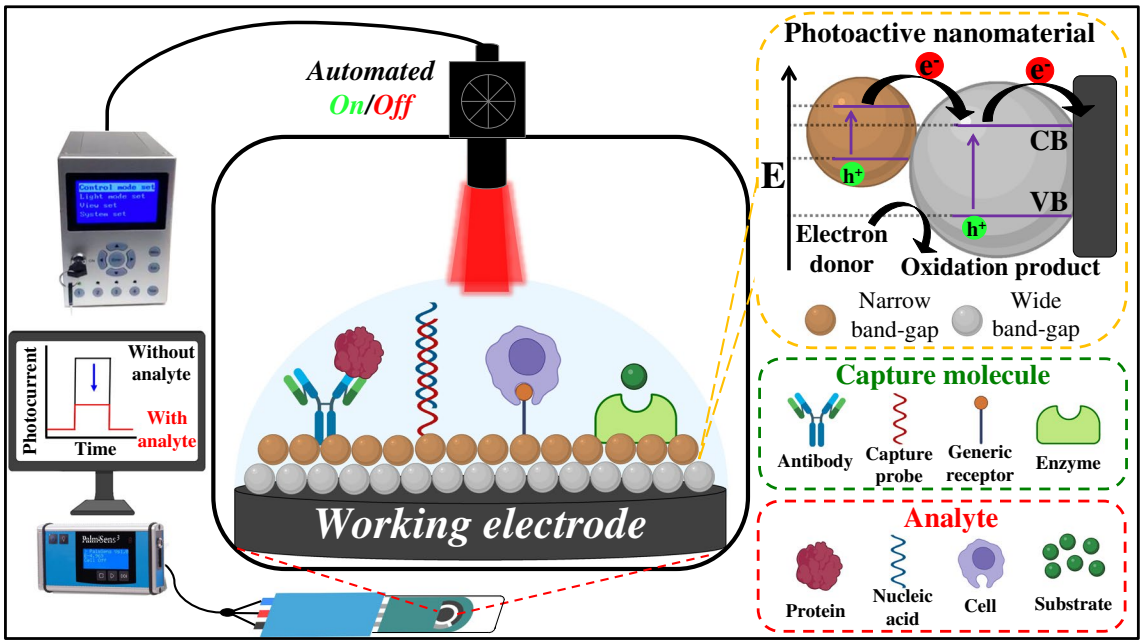

Fig. 1 Schematic representation of PEC assays utilizing miniaturized electrochemical cells, external excitation sources, and specific interactions in immunosensing, genosensing, enzymatic, and cytosensing assays. Charge generation and transduction occur at the electrode surface through photoactive nanomaterials promoted by the alignment of conduction (CB) and valence bands (VB) in materials with varying band-gaps

exposed surface area are related to the efficient transfer of charge carriers during reactions in electrolytic media [65].

Achieving proficient charge transfer and efficient electron flow within a PEC system hinges on the alignment of energy levels between photoactive nanomaterials and other components [66]. This alignment is crucial for effective charge injection, transport, and collection at the electrode. Equally important is selecting the appropriate excitation wavelength range and the energy level at which the nanomaterial is stimulated [67]. The range of wavelengths that photoactive nanomaterials absorb depends on their band-gap [68]. The feasibility of designing and manipulating this band-gap in PEC applications is demonstrated through doping, alloying, or quantum confinement effects. These methods allow absorption spectra adjustment and maximization of nanomaterial photoactivity [69].

Sources of signals and excitation

The photocurrent signals produced by PEC biosensors involve various kinetic and thermodynamic steps [70]. The performance of PEC biosensors is influenced by light excitation, photogenerated carrier transfer, and redox mechanisms [71, 72]. According to energy band theory, electrons are propelled from the valence band (VB) to the conduction band (CB) when photons with energy equal to or exceeding the band-gap energy (E_g) of the photoactive nanomaterial irradiate them [73]. These photogenerated carriers are then transported to the electrode or electrolyte, but their effective utilization requires their migration to the surface from within the material [74]. Upon the creation of the electron–hole pair, a fraction of carriers promptly recombines, while others do so during their journey to the surface (as illustrated in Fig. 1). Carrier migration, a relatively slow process, introduces varying recombination pathways. Upon reaching the surface, carriers might engage in redox reactions with electroactive species in the electrolyte [75]. Nonetheless, many carriers recombine on the surface before completing these processes due to the time-consuming nature of electroactive species adsorption and medium-related redox reactions. The migration of carriers and the rates of reactions in photoactive materials are influenced by the VB/CB levels and the redox potential of electroactive species [76]. From a thermodynamic standpoint, oxidation/reduction reactions occur when the oxidizing species potential is more positive than the CB level and the reducing species potential is more negative than the VB level [77].

(Bio)sensing formats and signaling strategies

The construction of PEC biosensing assays has proven challenging in developing novel photoactive nanomaterials and searching for more sensitive, precise, and accurate signals [78]. Highly specific and selective detection formats have achieved tests with minimal background noise compared to conventional methodologies [79]. The specificity and selectivity of the bioreceptor and the stable coupling with photoactive nanomaterials are paramount factors for direct detection of the molecular target [80, 81]. Consequently, PEC analysis's versatility and practical potential have found widespread applications in many scientific domains, particularly in identifying various (bio)analytes of biochemical and clinical interest [82]. These applications encompass nucleic acid analysis [44], immunoassays [83, 84], cell detection [85–87], enzyme and protein bio-detection [88–90], and monitoring of small (bio)molecules [91, 92].

Nevertheless, PEC detection presents a massive challenge in sensitively detecting various (bio)analytes, particularly those with exceedingly low levels, such as biomolecules, during the early stages of diseases. This reality places heightened demands on PEC sensors' sensitivity and detection range [11]. Therefore, numerous signal amplification strategies have been introduced to enhance the practical utility of the devices. High analytical performance, self-powered functionality, and miniaturization significantly impact the overall effectiveness of PEC detection systems [93]. Likewise, detecting multiple analytes and analyzing big data are other progressive needs that require customization of detection systems [94]. Consequently, the research on PEC biosensors has a noteworthy influence on endeavors to innovate and elevate the functionality of these devices [95, 96].

Classification of photoactive nanomaterials

Over the last decade, nanomaterials capable of interacting with electromagnetic radiation in the UV–visible and NIR ranges have been successfully coupled into PEC applications, highlighting photocurrent and photopotential signals [97, 98]. Table 1 overviews the critical characteristics of various materials used in PEC detection processes. PEC systems generally require a redox probe to reveal the generated photocurrent and complete the charge transport cycles. Most semiconductor systems used in PEC systems have well-defined band-gap values to determine the optimal excitation energy ranges. While band theory elucidates the general PEC principle, most PEC assays involve different optical and electrical phenomena depending on the nanomaterial and photoactive nanomaterials arranged on the transduction surface. In this context, molecular biorecognition events involve different PEC detection mechanisms. This review classifies PEC systems according to the photoactive nanomaterial type, including metals and metal oxides, carbon nitrides, quantum dots, semiconductors, and transition metal chalcogenides (TMCs).

Table 1 Classification of photoactive nanomaterials in UV- and visible-light-activated PEC biosensors

PEC materials	Platform structure	Electrolyte/redox probe	λ_{exc} (nm)	Band-gap (eV)	Detected biomarker	Linear range	LOD	Ref
Metals and metal oxides	Au@ZnO/FTO nanorods	GSH/GSSG–PBS	1 sun	-	GSH	20–1000 µM	3.29 µM	[99]
	ZnONRs/TNs/TiO	$(NH_4)_2SO_4$	≥420	2.89	AChE	0.05–1000 µM	0.023 µM	[100]
	$dTiO_{2-x}$@Au	Exo lll/PBS	585	2.52	DNA	1 pM–10 nM	0.6 pM	[101]
	Au/GR-CdS	Na_2SO_4	Xe Lamp	-	Diclofenac	1–150 nM	0.78 nM	[102]
	PdO/APFO-3:PCMB	$NaHCO_3$-PBS	1 sun	-	Oxygen	0.5–20 mg/L	0.034 mh/L	[103]
Carbon nitrides	g-C_3N_4/Co_3O_4	Na_2HPO_4/NaH_2PO_4	Xe lamp	2.62/2.13	Oxytetracycline	0.01 – 500 nM	3.5 pM	[104]
	g-C_3N_4/AuNPs/CoO	Na_2SO_4/PBS	>420	2.75/2.85	Microcystin-LR	0.1 pM – 10 nM	0.01 pM	[105]
	g-C_3N_4/$BiVO_4$	PBS	>420	2.70/2.40	Microcystin-LR	5 pg/L – 10 µg/L	41.9 fg/L	[106]
	g-CNS3	AA/PBS	Xe lamp	2.59	ALV-J	$10^{2.14}$–$10^{3.35}$ $TCID_{50}$/mL	$10^{2.08}$ $TCID_{50}$/mL	[107]
	g-C_3N_4/TiO_2	AAP/PBS	>460	2.69/3.21	Protein kinase A	0.05 – 100 U/mL	0.048 U/mL	[108]
Quantum dots	g-C_3N_4/CdS QDs	AA/PBS	Xe lamp	2.42	Prostatic antigen	0.01 – 50 ng/mL	4 pg/mL	[109]
	g-C_3N_4/CdS QDs	AA/NaCl-KCl	Xe lamp	2.42	MicroRNA-21	0.1 fM – 1 nM	0.05 fM	[110]
	rGO/CdS QDs	H_2O_2/PBS	>450	-	2,3′,5,5′ Tetrachlorobiphenyl	10–1000 ng/mL	1 ng/mL	[111]
	h-BN/CdS QDs	AA/PBS	Xe lamp	-	MicroRNA-141	0.001–100 nM	0.73 fM	[112]
	WS_2/β-CD@CdS nanorod	AA/PBS	1 sun	1.46/2.36	MicroRNA-21	0.1 fM – 10 pM	25.1 aM	[113]
Transition metal chalcogenides	Single-layer nanoMoS_2	PBS	White LED	-	Dopamine	10 pM – 10 µM	2.3 pM	[114]
	SnS_2@Ti_3C_2	Tris–HCl	Xe lamp	1.86	5cadCTP	0.001 – 200 nM	260 fM	[115]
	MoS_2/NGQDs	PBS	Xe lamp	-	Acetamiprid	0.05 pM – 1 nM	16.7 fM	[116]
	WS_2/MoS_2/β-TiO_2	AA/PBS	>420	1.37/1.57/2.38	5-Formylcytosine	0.01–200 nM	2.7 pM	[117]
	CdS/SnS_2/CNTs/GCE	PBS	Xe lamp	2.12/1.92	Hydroquinone	0.2–100 µM	0.1 µM	[118]

5cadCTP, 5-carboxy-2′-deoxycytidine-5′-triphosphate; *AA*, ascorbic acid; *AChE*, acetylcholinesterase; Ag_2S, silver sulfide; *AgI*, silver iodide; *ALV-J*, J avian leukosis virus; *APFO-3*, ammonium pentadecafluorooctanoate; *Au@ZnO/FTO*, heteroconjuction of gold nanoparticles, zinc oxide, and fluorine-doped tin oxide; *Au/GR-CdS*, heteroconjuction of gold nanoparticles, reduced graphene, and cadmium sulfide; *AuNPs*, gold nanoparticles; *BiOBr*, bismuth oxybromide; $BiVO_4$, bismuth vanadate; *BN*, boron nitride; *CdS QDs*, cadmium sulfide quantum dots; *CdS/SnS₂/CNTs/GCE*, heteroconjuction of cadmium sulfide, tin disulfide, carbon nanotubes, and glassy carbon electrode; *CN*, carbon nitride; *CoO*, cobalt(II) oxide; *DNA*, deoxyribonucleic acid; $dTiO_{2-x}$@*Au*, titanium dioxide and gold nanoparticles composite; *Exo III*, exonuclease III enzyme; $[Fe(CN)_6]^{3-/4-}$, hexacyanoferrate; *GSH*, glutathione; *GSSG*, oxidized glutathione; g-C_3N_4, graphitic carbon nitride; g-C_3N_4/Co_3O_4, heteroconjuction of graphitic carbon nitride and cobalt(II) oxide; *g-CNS3*, three-step thermal polycondensation of 2D g-C_3N_4 nanolayers; *ITO*, indium tin oxide; *KCl*, potassium chloride; *LOD*, limit of detection; $MgCl_2$, magnesium chloride; *MCF-7*, breast cancer cell line; MoS_2, molybdenum disulfide; Na_2SO_4, sodium sulfate; $NaHCO_3$, sodium hydrogen carbonate; $(NH_4)_2SO_4$, ammonium sulfate; *NGQDs*, nitrogen-doped graphene quantum dots; *PBS*, phosphate-buffered saline; *PCMB*, 4-chloromercuribenzoic acid; *PdO*, palladium oxide; *RNA*, ribonucleic acid; *rGO*, reduced graphene oxide; *S*, sulfur; SnS_2, tin(IV) sulfide; SnS_2@Ti_3C_2, heteroconjuction of tin (IV) sulfide and titanium carbide MXene; WS_2, tungsten disulfide; *Xe*, xenon; *ZnONRs/TNs/TiO*, heteroconjuction of zinc oxide nanorods and titanium dioxide; λ_{exc}, excitation wavelength

Metallic nanostructures are highly valued in PEC systems for their surface plasmon resonance properties, which enhance light-particle interactions and improve photoelectric conversion efficiency [119]. However, their high cost and potential toxicity are significant drawbacks. In contrast, metal oxides are known for their strong light absorption, adjustable energy band-gap, and exceptional chemical stability, making them suitable for harsh environments and effective at increasing photocurrent signals, although they may suffer from charge carrier recombination losses [120]. On

the other hand, carbon nitrides (g-C_3N_4) offer high chemical stability and ease of functionalization due to their two-dimensional (2D) structure and carbon–nitrogen conjugated bonds, but their relatively low conductivity can be a limitation [121]. Conversely, semiconductor quantum dots are appreciated for their quantum confinement effects, which enable size-tunable optoelectronic properties and efficient charge transfer [122]. However, they can encounter stability and toxicity issues. Finally, TMCs exhibit diverse optoelectronic properties and can function as metals and semiconductors, depending on their structure and conditions. They offer significant potential but face challenges with defect control and complex material synthesis [123].

Each type of nanomaterial has unique advantages and drawbacks, influencing its suitability for specific PEC applications. The properties of each photoactive nanomaterials play a crucial role, individually or as composite nanomaterials, in the assembly of biosensor platforms. These platforms leverage the unique virtues of each nanomaterial to enhance the detection device's analytical properties. The selection of the spectral range of radiation in the PEC process depends on the wavelength at which each photoactive material in the platform absorbs the radiation and uses it in the PEC detection process. The following section briefly reports the mechanisms explored for each family of materials.

Metals and metal oxides

The use of metallic nanostructures, such as those based on Au, Ag, and platinum (Pt), has been prompted in PEC systems due to their surface plasmon resonance properties [124]. Plasmons entail the collective oscillations of electrons on the surface of metallic nanoparticles. Electrons are excited when light interacts with these nanoparticles, generating plasmonic oscillations that produce a distinctive light-particle interaction [125]. This interaction leads to surface plasmon resonance, wherein light gets absorbed and scattered at particular wavelengths [126]. Plasmonic metal nanostructures can interact with light at frequencies aligned with the coherent oscillation of conduction electrons on the nanostructure's surface, thus generating resonant surface plasmons [127–129]. Excitation with wide energy ranges favors the injection of hot electrons into the conduction bands of semiconductor materials through metal resonant plasmon energy transfer. The versatile optoelectronic attributes of plasmonic nanoparticles (narrow band-gap) enable photoelectric conversion efficiency through intimate interaction with wide band-gap semiconductors [130, 131].

Metal oxides constitute a class of nanomaterials with semiconducting characteristics ideal for applications in PEC devices. Metal oxides present strong light absorption, modulable charge carriers (electrons and holes), and extensive surface area available for electrocatalytic reactions [132, 133]. Metal oxides have broad and tunable energy band-gap, which allow them to absorb radiation in a wide range of wavelengths, a fundamental characteristic for generating electrons and holes upon material illumination [134]. Likewise, metal oxides have exceptional chemical stability and are suitable for operating in corrosive or hostile environments, such as PEC cells [135, 136]. Many metal-oxide nanomaterials have catalytic properties, accelerating electrochemical reactions and increasing photocurrent signals [137].

Zhang et al. [99] conducted a glutathione detection assay utilizing a "photo-anode" founded on zinc oxide (ZnO) nanorods decorated with Au nanoparticles. This plasmonic nanoparticle/semiconductor hybrid was employed as a comparative and competitive test to elucidate the role of metallic nanoparticles as charge transducers induced by the injection of hot electrons into the ZnO conduction band. Investigating the pathways of PEC signaling was based on water oxidation, the reaction's self-sustaining capability, and the detection of various glutathione concentrations. Figure 2 *A* illustrates the detection mechanism of the Au/ZnO hybrid interface, where the surface plasmon resonance (SPR) of the Au nanoparticles enhances the absorption of visible plasmon-induced irradiation, generating energetic hot electrons. These electrons are then transferred to the conduction band of the metallic oxide material, facilitating charge transfer at the working electrode and enhancing charge carrier separation. Leveraging the surface sensitization provided by Au nanoparticles enables the creation of a glutathione disulfide (GSSG) detection assay with a linear range of 20–1000 μM, $R^2 = 0.996$, and a LOD of 3.29 μM across the entire spectral window, encompassing both visible and ultraviolet ranges.

Conversely, the utilization of titanium oxide (TiO_2) [10, 138] and its anatase phase (β-TiO_2) [101] (Fig. 2B) has been explored for detecting specially designed DNA sequences within photoelectrode arrays. The plasmonic effect of an AuNP/tDNA nanobioconjugate on $dTiO_{2-x}$ was employed for PEC detection of DNA. Likewise, exonuclease III (Exo III)-assisted target recycling amplification was coupled to the detection system to amplify the number of rDNA segments labeled with AuNPs. The capture probe targeted DNA sequences related to the manganese superoxide dismutase gene (MnSOD gene), a regulator of cellular redox homeostasis. AuNP-tagged hairpin DNA probes were designed to recognize target DNA (tDNA) and undergo hybridization, activating Exo III and leading to the digestion of the probes into residual DNA (rDNA) segments containing AuNPs. These segments were then anchored to the electrode surface, facilitating DNA analysis. When plasmonic nanoparticles and TiO_2 converged within approximately 10 nm or less, a direct influence on the lifespan of charge carriers was observed. The generated hot electrons with a higher negative potential than that of the CB of $dTiO_{2-x}$ could be injected smoothly

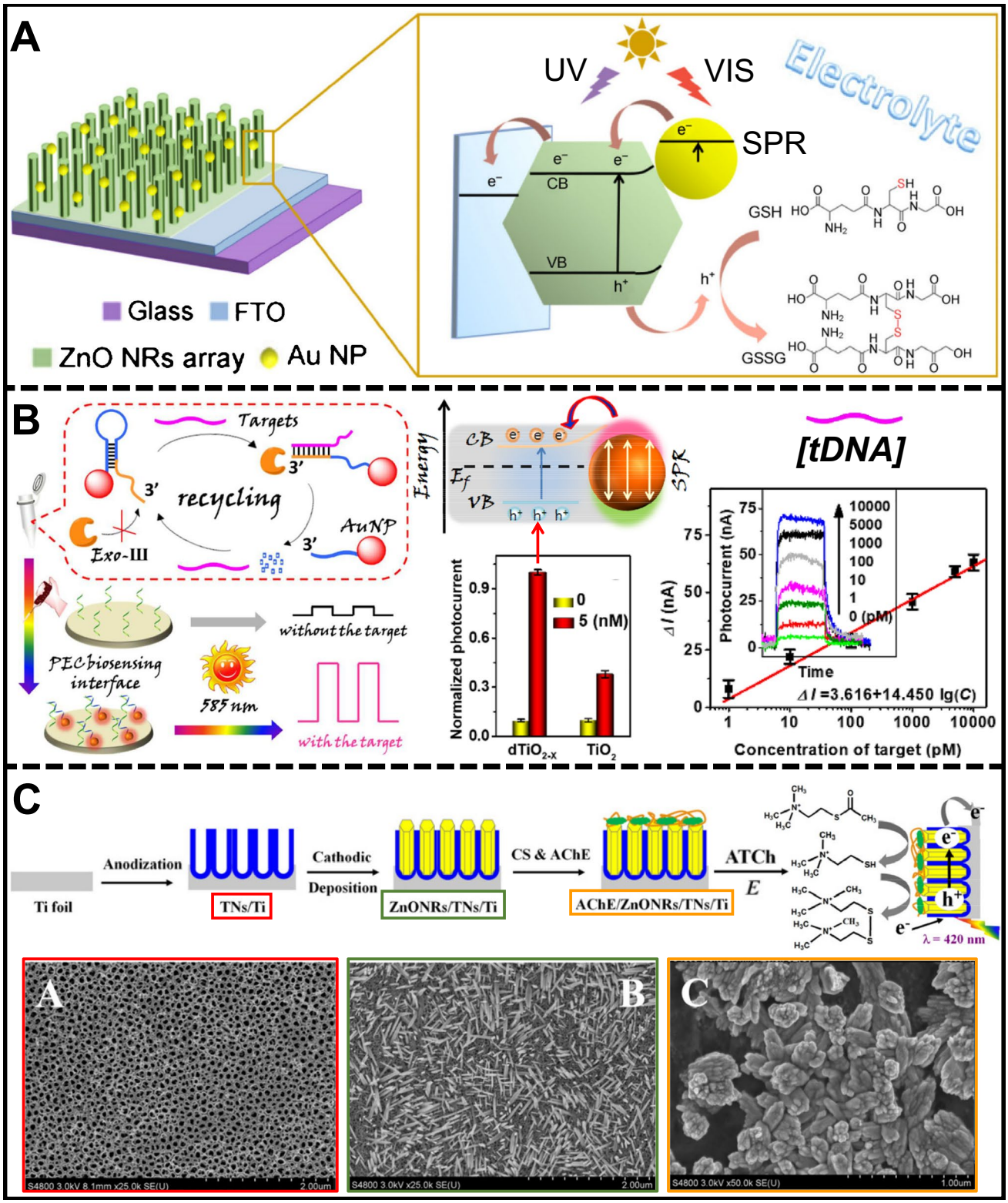

Fig. 2 **A** Au/ZnO hybrid interface for PEC detection of GSSG, reproduced with permission from Ref. [99]. **B** PEC genosensor system based on $dTiO_{2-x}$-AuNPs interaction for tDNA detection, reproduced with permission from Ref. [101]. **C** Fabrication of a PEC enzymatic sensor for elucidating the activity of AChE, reproduced with permission from Ref. [100]

into the CB, resulting in the enhancement of photocurrent. Moreover, the impact of the crystalline phase of TiO_2 was demonstrated with a LOD of 0.6 pM, a linear range between 1 pM and 10 nM, and a high linearity ($R^2 = 0.967$). This effect was rooted in the interplay between the nanomaterial structure of PEC processes and surface plasmons' resonance, together with the injection of hot electrons into the semiconductor's conduction band [139].

Zhang et al. [100] utilized a label-free PEC biosensing method to study acetylcholinesterase (AChE) activity using a nanocomposite made of zinc oxide nanorods (ZnONRs) within titanium dioxide nanotubes (TNs) on titanium foils (Fig. 2C). The PEC nanocomposite was created by anodic oxidation of Ti foil to form TNs, followed by cathodic deposition of ZnONRs. AChE immobilized on this nanocomposite showed enhanced photoelectrochemical responses under visible light. They observed that high concentrations of Cd^{2+} inhibited AChE activity, while low levels stimulated it. The PEC assay produced electron holes under light irradiation, which reacted with acetylthiocholine (ATCh) to generate thiocholine (TCh). It increased the photocurrent proportionally to the TCh concentration, reflecting AChE activity. The assay demonstrated high linearity in the 0.05–1000 µM range with a LOD of 0.023 µM. This method aided in understanding how metal ions affect enzyme activity and the pathogenesis of neurodegenerative disorders.

Carbon nitrides

Carbon nitrides are 2D nanostructures, often called g-C_3N_4, bearing a graphitic-like framework constituted by carbon and nitrogen atoms intricately assembled within a singular crystal lattice [140]. Their layered, planar configuration facilitates the establishment of carbon–nitrogen conjugated bonds, fostering the generation of a continuous network of delocalized electrons traversing the 2D structure and conferring semiconductor attributes [141]. This distinctive feature was harnessed by Zeng et al. [142], who devised a photoelectrode based on graphitic carbon nitride, silver, and silver iodide (g-C_3N_4/Ag/AgI) heterojunction, as illustrated in Fig. 3A. The integration of 2D g-C_3N_4 nanostructure with Ag as a plasmonic metal facilitated the design of a highly selective detection assay for hydrogen sulfide (H_2S). The interaction of band-gap values, ranging between 2.7 eV (g-C_3N_4) and 2.8 eV (Ag/AgI), along with the strategic alignment of AgNPs, catalyzed electron transfer across metal/metal iodide and carbon nitride domains. The distribution of the three components on the platform formed a Z-scheme type system that reduced the recombination of photogenerated electron–hole pairs. The gradually increasing photocurrent showed that the Z-scheme pathway efficiently promoted the photoelectric conversion efficiency of g-C_3N_4. In the presence of target S^{2-}, the AgI was transformed to Ag_2S, leading to the broken Z-scheme electron migration pathway and, thus, the decreased photocurrent. The authors established that a 402-nm monochromatic radiation source was optimal for inducing the generation of hot electrons in plasmonic metals, their subsequent transfer to the 2D structure, and the acceleration of delocalized electrons. The optimal Z-scheme junction led to a highly effective PEC detection assay, exhibiting linearity between 5 and100 µM ($R^2 = 0.998$) and a LOD of 1.67 µM. This phenomenon stemmed from the judicious selection of the excitation range, a facet substantiated by spectroscopic analyses performed on the photoelectrode [143].

The research of Xu et al. [144] also exploited the characteristics of an interface of g-C_3N_4 and α-Fe_2O_3 (Fig. 3B). This strategic pairing engendered a heterojunction for rapid migration of photogenerated carriers, thereby increasing the overall efficiency. The electrons within α-Fe_2O_3 could be effectively roused toward the conduction band, leveraging the influence of a 390-nm monochromatic radiation source to incite a gap formation within the valence band. Subsequently, the energized electron underwent a process of resonance energy transfer to the nanostructure of g-C_3N_4. The delocalized electrons gained momentum within this domain, participating in redox reactions in the medium. This assay highlighted the electron acceptor attributes inherent to graphitic carbon nitride structures, demonstrating high linearity ($R^2 = 0.993$) in the range of 0.1–11.5 mg/L and a LOD of 0.03 mg/L. Combining g-C_3N_4 with other semiconducting or metallic materials produced exceptional photoactive nanocomposites ideal for supporting PEC detection assays [145].

Tan et al. [105] developed an aptamer-based PEC sensor (aptasensor) and a heterojunction composed of cobalt oxide (CoO), AuNPs, and g-C_3N_4 to detect microcystin-leucine arginine (MC-LR). The PEC platform, shown in Fig. 3C, enhanced the separation of photo-induced electron–hole pairs, and AuNPs significantly increased the visible light absorption through SPR. The heterojunction structure benefited from the large surface area of g-C_3N_4 and the tailored band-gap between g-C_3N_4 and CoO. AuNPs at the CoO-g-C_3N_4 interface enhanced light absorption and acted as electron mediators, forming a Z-scheme-type system that reduced charge carrier recombination. When MC-LR was captured on the PEC aptasensor, holes accumulated on the CoO VB, oxidizing MC-LR and further hindering electron–hole recombination, resulting in increased photocurrent. Visible light irradiation generated electrons on the CoO CB that flow to AuNPs, recombining with holes from the g-C_3N_4 VB, enhancing electron–hole pair separation and suppressing recombination. The SPR effect of AuNPs also produced hot electrons, contributing to increased photocurrent for MC-LR quantification, with a linear range of 0.1 pM to 10 nM, an $R^2 = 0.997$, and a low LOD of 0.01 pM.

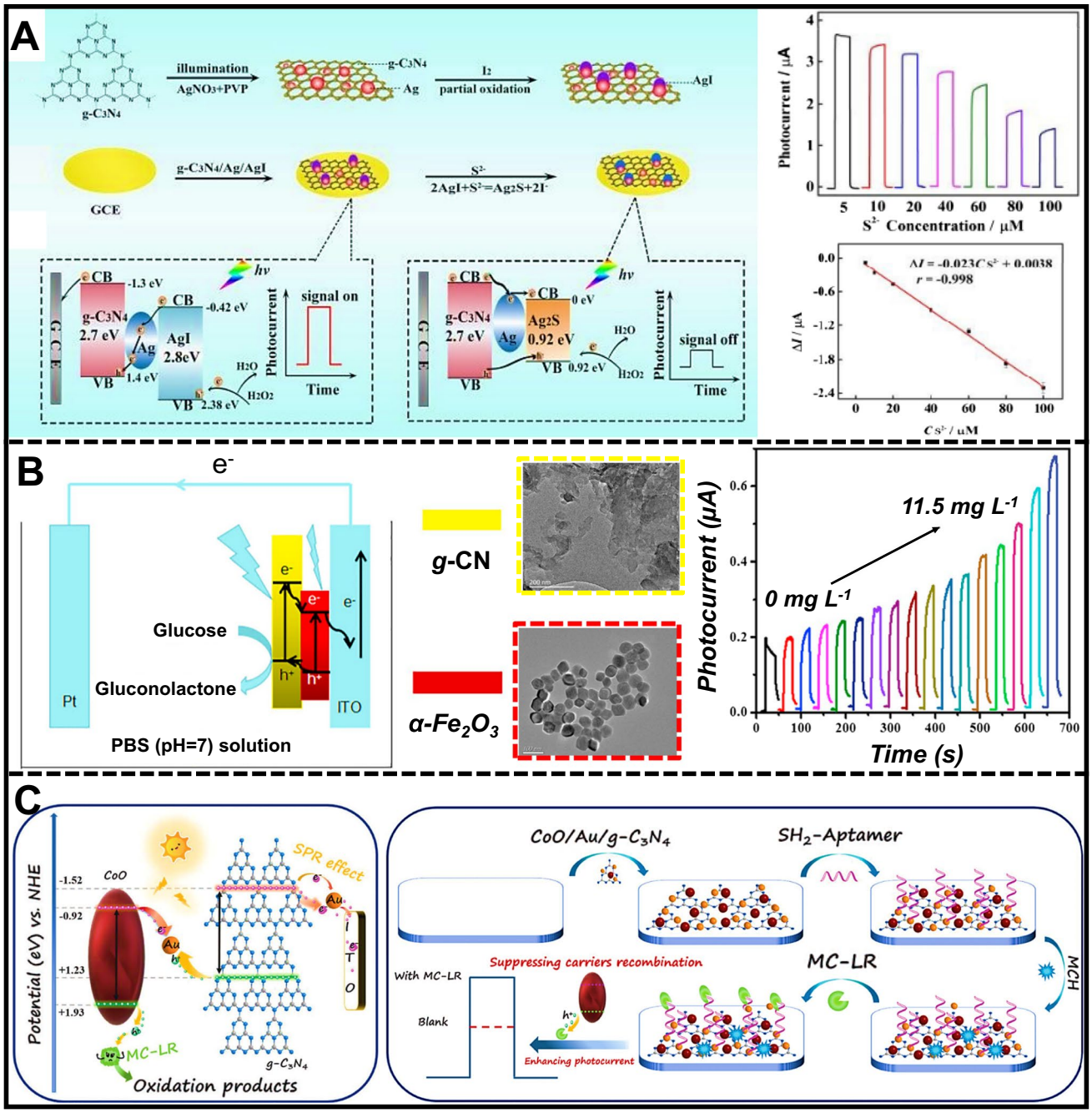

Fig. 3 **A** GCE/g-C_3N_4/Ag/AgI assembly for the PEC detection of S^{2-} mean the Ag_2S formation, reproduced with permission from Ref. [142]. **B** g-C_3N_4/α-Fe_2O_3/ITO heterojunction for the PEC detection of glucose, reproduced with permission from Ref. [144]. **C** PEC aptasensor assembly based on CoO/Au/g-C_3N_4 heterojunction for the MC-LR detection, reproduced with permission from Ref. [105]

Quantum dots (QDs)

Semiconductor QDs constitute a collection of nanoscale materials, typically encompassing 10^2–10^5 atoms, with dimensions not exceeding 10 nm [146, 147]. Their compactness engenders an environment conducive to the quantum confinement of electrons and holes across all three spatial dimensions [148]. Consequently, QDs harbor a distinctive semiconductor property wherein the energies and wave functions of the constrained quantum states can be manipulated by adjusting the QDs' size, shape, and composition. This inherent confinement is pivotal for exceptionally efficient charge transfer [149, 150].

Xue et al. [113] demonstrated the PEC behavior of QDs using a photoelectrode composed of tungsten disulfide (WS_2), β-cyclodextrin (β-CD), and cadmium sulfide (CdS)

heterostructure (Fig. 4A). Incorporating CdS QDs increased the photocurrent due to their ability to generate holes and electrons, which were enhanced by quantum confinement effects and created a localized electric field for ascorbic acid (AA) oxidation. The experiment used a variable power radiation source covering the visible spectrum and specific ultraviolet frequencies, highlighting the narrow wavelength activation range of QDs. The nanostructured interface was utilized to construct an ultrasensitive PEC biosensor for detecting microRNA-21 (miR-21) using a cyclic strand displacement reaction (SDR)-mediated Cu^{2+} quenching mechanism. Adamantane (ADA)-labeled hairpin DNA1 (ADA-H1) was immobilized on the electrode via host–guest interaction with β-CD@CdS. When a mixture of target miR-21 and biotin-labeled hairpin DNA2 (Bio-H2) was added, ADA-H1 unfolded through hybridization. Bio-H2 then hybridized with ADA-H1, releasing miR-21 and triggering another SDR process. Avidin-labeled CuO nanoparticles attached to the duplex were dissolved, releasing Cu^{2+}, which reacted with CdS to form Cu_xS, reducing the photocurrent. This easy-to-assemble WS_2/β-CD@CdS heterojunction and the SDR-dependent Cu^{2+} quenching signal cascade enabled highly sensitive miR-21 detection, with a highly linear range of 0.1 fM to 10 pM ($R^2 = 0.997$) and a LOD of 25.1 aM.

In a similar vein, Liu et al. [109] developed a label-based PEC biosensing method for detecting prostate-specific antigen (PSA) using a CdS@g-C_3N_4 heterojunction and CuS-conjugated antibodies (Ab_2-CuS) for signal amplification (Fig. 4B). The PEC immunosensor was constructed by assembling CdS@g-C_3N_4, chitosan (CS), AuNPs, and primary antibodies (Ab_1) on dual electrodes, followed by blocking unbound sites with bovine serum albumin (BSA). Varying concentrations of PSA were added to one working electrode (WE1) and a fixed concentration to the other (WE2) before incubating Ab_2-CuS on both. The specific binding of PSA to Ab_2-CuS led to a weakened photocurrent response in a linear concentration range of 0.01–50 ng/mL and a LOD of 4 pg/mL. Spatial resolved radiometry was based on the photocurrent intensity ratio between WE1 and WE2. With well-matched band energies, the photoactivity of the CdS core and g-C_3N_4 shell enabled effective light harvesting and electron–hole pair separation. Electrons migrated to the CdS CB while holes transferred to the g-C_3N_4 VB, enhancing photoactivity and stability. The Ab_2-CuS conjugates acted as signal amplifiers by weakening the PEC intensity in the presence of PSA. This effect occurred due to photogenerated electrons transferring from g-C_3N_4 to CuS, reducing electron transfer to the electrode. The captured electrons formed $O_2^{-\bullet}$ with dissolved O_2, enabling ultrasensitive PSA detection through photocurrent generation.

QDs coupled to highly sensitive and label-free PEC biosensors were also studied by Yu et al. [112], as shown in Fig. 4C. The PEC biosensor was based on CdS QDs sensitized porous hexagonal boron nitride (h-BN) nanosheets (NSs) and multiple-site tripodal DNA walkers (TDWs) formed through catalytic hairpin assembly (CHA). The porous h-BN NSs provided a large surface area and numerous active sites, making them ideal for photoelectric substrate materials. The h-BN/CdS QDs composite ensured the efficient transmission of photogenerated electrons and holes, resulting in high photoelectric conversion efficiency. CHA-formed TDWs triggered by miRNA-141 immobilized a significant amount of alkaline phosphatase (ALP) on the electrode surface, catalyzing ascorbic acid 2-phosphate (AAP) to produce AA as an electron donor. The h-BN/CdS QDs composite was coupled to a fluorine-doped tin oxide (FTO) electrode and modified with Hairpin4 (H4) DNA tracks. Upon miRNA-141 initiation, TDWs bound to H4 on the electrode surface and underwent strand displacement, exposing the toe region of H4. This region formed a double-stranded DNA structure with ALP-AuNPs-H5 through further strand displacement, continuing the walking process and anchoring more ALP on the electrode. Under visible light, h-BN NSs and CdS QDs photogenerated electrons and holes, moving electrons from the CB of h-BN to CdS QDs and then to the electrode, creating a stable photocurrent. It allowed for the sensitive detection of miRNA-141, achieving an excellent linear range from 1 fM to 100 nM ($R^2 = 0.997$) and a detection limit of 0.73 fM. This PEC biosensor provides a robust strategy for early clinical diagnosis and biomedical research.

Transition metal chalcogenides (TMCs)

TMC nanomaterials are composed of chalcogen atoms, commonly oxygen, sulfur, selenium, or tellurium, in conjunction with a transition metal [151, 152]. Extensive research has been conducted to explore the optoelectronic properties of TMCs, especially tungsten disulfide (WS_2) and MoS_2. The molecular arrangement of TMCs involves positioning metal atoms surrounded by chalcogen atoms in an organized manner, forming 2D or 3D layers [153]. Due to the specific arrangement of atoms within the structure, they can exhibit conductive characteristics under certain conditions, such as nanometer-scale thinning or introducing defects [154, 155].

Wang et al. [156] and Dai et al. [116] reported improved performance of TMCs through the synergy of MoS_2/N-graphene (Fig. 5A) and MoS_2/NGQDs (Fig. 5B) nanostructures, respectively. Both studies utilized semiconductors to sensitize the TMCs and capture signals within narrow wavelength ranges of approximately 400 and 630 nm. Wang et al. employed MoS_2/N-graphene (NGH) heterojunctions for PEC analysis of chloramphenicol (CAP) in food samples with the aid of a CAP aptamer. The MoS_2/NGH composites displayed a reversed "V-shaped" p-n heterojunction curve, promoting efficient

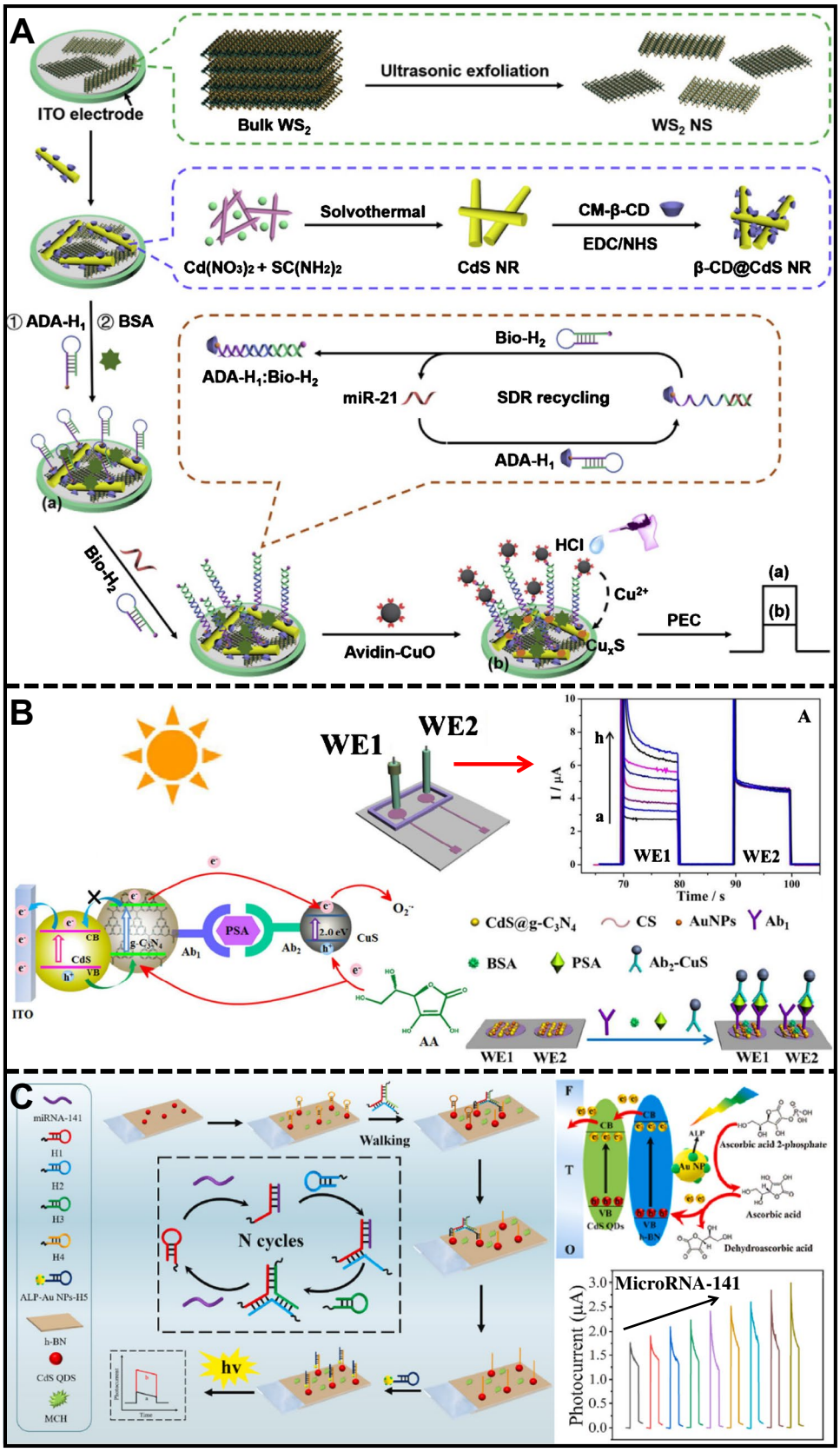

Fig. 4 **A** WS_2/β-CD@CdS assembly for the PEC detection of miR-21, reproduced with permission from Ref. [113]. **B** PEC immunosensor based on ITO/CdS/g-C_3N_4/CuS heterojunction for the PSA detection, reproduced with permission from Ref. [109]. **C** FTO/CdS/h-BN/AuNPs heterojunction platform for the PEC detection of miRNA-141, reproduced with permission from Ref. [112]

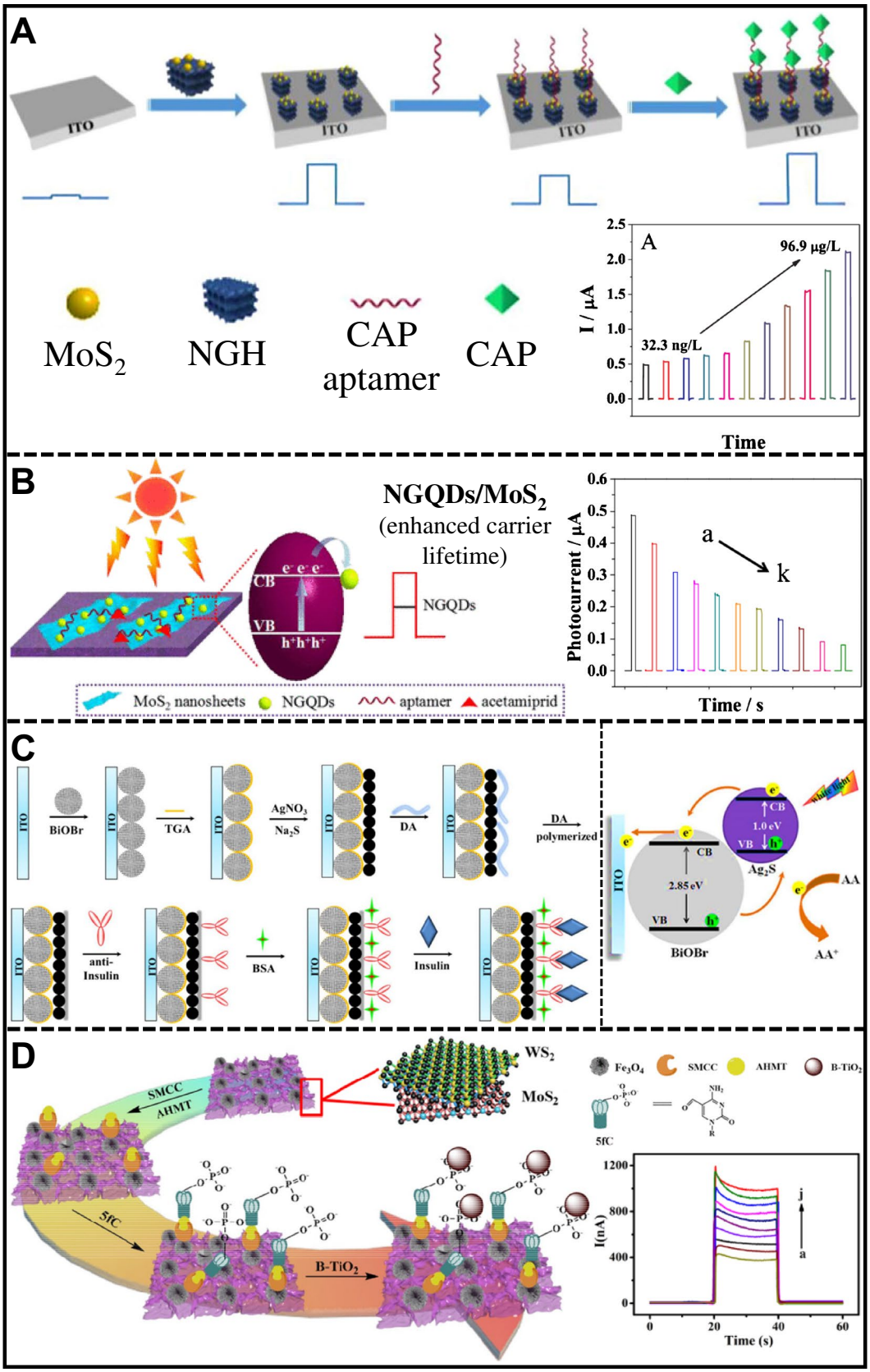
A
ITO
MoS2
NGH
CAP aptamer
CAP
A
96.9 μg/L
32.3 ng/L
I / μA
Time
B
NGQDs/MoS2
(enhanced carrier lifetime)
CB
VB
NGQDs
MoS2 nanosheets
aptamer
acetamiprid
Photocurrent / μA
a
k
Time / s
C
BiOBr
TGA
AgNO3
Na2S
DA
DA polymerized
anti-Insulin
BSA
Insulin
CB
1.0 eV
VB
Ag2S
2.85 eV
BiOBr
AA
AA+
D
WS2
MoS2
SMCC
AHMT
Fe3O4
B-TiO2
5fC
I(nA)
Time (s)
j
a

◂**Fig. 5** **A** PEC aptasensor based on ITO/NGH/MoS_2 for CAP detection, reproduced with permission from Ref. [156]. **B** MoS_2/NGQDs-modified platform for PEC aptasensing detection of acetamiprid, reproduced with permission from Ref. [110]. **C** PEC immnosensing assembly for insulin detection based on ITO/BiOBr/Ag_2S heterojunction, reproduced with permission from Ref. [157]. **D** WS_2/MoS_2/Fe_3O_4/β-TiO_2 platform for PEC detection of 5fC, reproduced with permission from Ref. [117]

spatial charge separation and longer photocarrier lifetimes. The PEC sensor recognized CAP quickly, inhibiting electron–hole recombination and enhancing the photocurrent. The sensor showed excellent linearity from 32.3 ng/L to 96.9 µg/L ($R^2 = 0.998$), with a detection limit of 3.23 ng/L. On the other hand, Dai et al. used nitrogen-doped graphene quantum dots (NGQDs) with ultrathin MoS_2 nanosheets (NGQDs/MoS_2) to create a high-performance photoactive material. The NGQDs extended the lifetimes of photogenerated charge carriers, leading to improved charge separation and substantial photocurrent signal amplification for acetamiprid detection. The photocurrent intensity decreased with increasing acetamiprid concentration, showing a linear range from 0.05 pM to 1 nM and a detection limit of 16.7 fM. These advancements highlight the benefits of TMCs in PEC detection, including chemical stability, efficient charge carrier separation, and transport, resulting in significantly improved detection performance.

One particular type of TMC is metal sulfides, a class of nanomaterials that manifest metallic and semiconductor properties ideal for electronic applications [158, 159]. The optoelectronic mechanism of these materials hinges on the role of metal cations as electron donors and sulfide anions as electron acceptors [160], resulting in a partially occupied valence band and an unoccupied conduction band. This dynamic engenders a distinctive band-gap contingent upon the structural attributes of the ionic arrangement within the crystal lattice [11, 161]. One clear example is given by Wei et al. [157]. They developed a highly sensitive insulin detection assay on bismuth oxybromide (BiOBr) and silver sulfide (Ag_2S)-modified indium tin oxide (ITO) electrodes (Fig. 5C). The photoelectrode was irradiated with 420-nm monochromatic light in a solution with AA as a redox probe and PBS as an electrolyte medium. The resonant energy levels of the BiOBr microspheres and Ag_2S nanoparticles enabled efficient electronic transition under visible light with high photocurrent signals compared to the individual systems. The photocurrent response in the PEC system decreased with a progressive increase in the insulin concentration on the electrode in a range between 0.001 to 20 ng/ml, $R^2 = 0.993$, and a detection limit of 0.2 pg/ml. This method ensured measurement stability and robust PEC activity.

Likewise, ITO photoelectrodes were modified with a heterojunction of nanosheets of tungsten disulfide, molybdenum disulfide, and titanium dioxide (WS_2/MoS_2/β-TiO_2) to detect 5-formylcytosine (5fC), as shown in Fig. 5D [117]. The nanostructured surface of TMCs was coated with Fe_3O_4-NH_2 covalently coupled to 4-amino-3-hydrazino-5-mercapto-1,2,4-triazole (AHMT) using a cross-linker of N-succinimidyl 4-(N-maleimidomethyl) cyclohexanecarboxylate (SMCC). The hydrazine of AHMT specifically captured 5fC by reaction with the aldehyde groups of the AHMT/Fe_3O_4/WS_2/MoS_2/ITO interface. AA was used as a redox probe for interference-free detection under white light. 2D metal sulfide-semiconductor heterojunctions demonstrated outstanding photoactive and analytical performance, with a linear range of 0.01–200 nM ($R^2 = 0.998$) and a LOD of 2.7 pM. It highlights the role of TMCs in PEC sensing applications, providing sensitive and time-stable responses.

In the evolving field of PEC bioanalysis, significant progress has been made across various approaches and applications, each offering unique advantages and challenges. Zhao et al. [42] emphasized integrating PEC techniques with biomolecular detection, highlighting the development of bismuth-based photoelectrodes to address toxicity and low efficiency in conventional materials. This approach shows promise in enhancing PEC performance through improved charge separation and light absorption. On the other hand, Ai et al. [43] focused on applying electrochemical, electrochemiluminescent, and PEC techniques for detecting epigenetic modifications, underscoring the importance of these methods in diagnosing diseases and understanding biological functions. It emphasized the need for ultra-sensitive and specific detection technologies in this context. Similarly, Chen et al. [44, 45] provided an extensive overview of PEC DNA biosensors, detailing the types of transducers and probe immobilization techniques used and various DNA interactions that can be monitored. Despite significant advancements, challenges such as stability and reproducibility remain, with future research directed to solve such issues, develop new photoactive materials, and integrate nanotechnology for clinical applications.

Liu et al. [162] explored the advancements in self-powered PEC sensors, which enhance portability and simplify operation by eliminating the need for external power sources. These sensors leverage solar energy to drive redox reactions, offering superior sensing performance and environmental benefits. In contrast, Pang et al. [163] delved into semiconductor nanomaterial-based PEC biosensing, highlighting the role of materials such as metallic oxides, sulfides, and graphitic carbon nitride in constructing high-performance PEC sensors. It pointed out the challenges of improving photoconversion efficiency and addressing photobleaching. Finally, Tang et al. [79] emphasized the impact of nanotechnology on PEC biosensing, focusing on advanced photoactive nanomaterials and their charge separation and transfer mechanisms, the biomedical applications of PEC biosensors, and the potential of composite materials

in overcoming limitations like high charge recombination rates and low photoelectric conversion efficiency. Overall, the promising future of PEC bioanalysis, driven by continuous innovations in material science and sensing mechanisms, aims to enhance sensitivity, specificity, and practical applications in fields ranging from disease diagnosis to environmental monitoring.

Red light and NIR excited PEC biosensors

The evolution of diverse structural configurations integrating optical and electrochemical analyses sets the stage for the refinement of more accurate and efficient PEC assays to quantify a wide array of substances [164]. Within this framework, the adoption of red light and NIR excitation in PEC devices offsets the limitations of existing sensors with UV light. Radiation in the UV range restricts the applications of PEC biosensors in areas of biodetection of clinically relevant biomarkers due to conformational damage and decreased biological activity of protein-type bioreceptors such as antibodies or enzymes [165–167]. NIR light, spanning wavelengths from over 650 up to 1700 nm, is gaining importance in biosensing and biomedicine due to its minimal spectral interference, ability to penetrate deep tissues, and limited harm to biological entities [168, 169]. Consequently, considerable efforts have been devoted to extending the excitation source into the visible spectrum by coupling small band-gap semiconductors to augment light absorption efficiency and biosensor performance. Radiation in this range is less energetic, facilitating non-invasive or minimally invasive detection in biological samples such as blood or tissues [170, 171]. Red light and NIR PEC biosensors also exhibit reduced background interference (photobleaching), which improves signal quality, biosensor sensitivity, and probe stability over extended analysis periods [172]. Table 2 reviews the most representative reports on nanobiosensors activated by red and NIR light.

Red and NIR light have been explored to detect breast cancer cell lines (MCF-7) [173, 174]. Plasmonic nanoparticles were incorporated into ITO electrodes modified with multicomponent semiconductor nanomaterials to improve the photoelectric conversion efficiency. In the first study, TMC, WS_2, and AuNPs heterojunctions were assembled on ITO to detect MCF-7 cells non-invasively. A long excitation

Table 2 PEC biosensors activated by red light and NIR

Platform structure	Electrolyte/redox probe	λ_{exc} (nm)	Detected biomarker	Linear range	LOD	Ref
ITO/WS_2/AuNPs	PBS/AA	630	MCF-7 cell	10^2 –5×10^6 cells/mL	21 cells/mL	[173]
ITO/AgS_2/AuNPs	PBS/AA	810	MCF-7 cell	10^2 – 10^7 cells/mL	100 cells/mL	[174]
FTO/$NaYF_4$:Yb,Tm@TiO_2	G bases	980	CEA	0.01–40 pg/mL	3.6 pg/mL	[175]
GC/AuNSs	PBS	780	AA	0.1 – 11 mM	10 µM	[176]
ITO/Bi_2O_2S/AuNPs	PBS/AA	808	MCF-7 cell	50 – 5×10^6 cells/mL	17 cells/mL	[177]
FTO/$NaYF_4$:Yb,Tm/ZnO/CdS	PBS/AA	980	AFP	0.01–200 ng/mL	5 pg/mL	[178]
FTO/CdS/$NaYF_4$:Yb,Tm@$NaYF_4$	PBS	980	miRNA-21	0.05–100 nM	8 pM	[179]
FTO/Ag_2S/AuNP	PB	980	MC-LR	10 pg/L –10 µg/L	7 pg/L	[180]
ITO/$AgInS_2$	Tris–HCl/AA-NaCl-KCl	630	CCRF-CEM cell	1.5×10^2–3×10^5 cells/mL	16 cells/mL	[56]
$NaYF_4$:Yb,Tm@ZnO	Na_2SO_4	980	CEA	0.1–300 ng/mL	0.032 ng/mL	[181]
$NaYF_4$:Yb,Er/Ag_2S	Na_2SO_4	980	CEA	0.005–5 ng/mL	1.9 pg/mL	[165]
TiO_2/AuNPs	PBS	760	TET	2–150 nM	0.6 nM	[182]
ITO/CN/TsCuPc	PB/DA	> 630	DA	0.05–50 µM	2 nM	[183]
FTO/ZnO/Ag/$NaYF_4$:Yb,Tm	PBS	980	AFP	0.05–100 ng/mL	0.04 ng/mL	[184]
$NaYF_4$:Yb,Er@CdTe	Na_2SO_4	980	CEA	10 pg/mL – 5.0 ng mL	4.8 pg/mL	[185]
FTO/$NaYF_4$:Yb, Er@Au@CdS	Na_2SO_4/glucose-H_2O_2	980	AFP	0.01–40 ng/mL	5.3 pg/mL	[186]

AFP, alpha-fetoprotein; *AuNSs*, gold nanostars; *AA*, ascorbic acid; *$AgInS_2$*, silver indium disulfide quantum dot; *AgS_2/AuNPs*, heteroconjuction of silver sulfide quantum dot and gold nanoparticles; *Bi_2O_2S/AuNPs*, heteroconjuction of bismuth oxysulfide chalcogenide and gold nanoparticles; *CEA*, carcinoembryonic antigen; *CN/TsCuPc*, heteroconjuction of carbon nitride and copper phthalocyanine; *DA*. dopamine; *FTO*, fluorine-doped tin oxide; *G*, guanine; *GC*, glassy carbon; *H_2O_2*, hydrogen peroxide, *ITO*, indium tin oxide; *KCl*, potassium chloride; *λ_{exc}*, excitation wavelength; *miRNA-21*, microRNA 21; *Na_2SO_4*, sodium sulfate; *NaCl*, sodium chloride; *$NaYF_4$, Er@CdTe*, core–shell sodium yttrium tetrafluoride doped with ytterbium and erbium, coated with cadmium telluride upconversion nanoparticle; *$NaYF_4$, Tm@TiO_2*, core–shell sodium yttrium tetrafluoride doped with ytterbium and thulium, coated with titanium dioxide upconversion nanoparticle; *$NaYF_4$, Tm/ZnO/CdS*, heteroconjuction of sodium yttrium tetrafluoride doped with ytterbium and thulium upconversion nanoparticle, zinc oxide, and cadmium sulfide; *PB*, phosphate-buffered; *PBS*, phosphate-buffered saline; *TET*, *Tris–HCl*, Tris(hydroxymethyl)aminomethane hydrochloride; *WS_2/AuNPs*, heteroconjuction of tungsten disulfide and gold nanoparticles

wavelength was employed in PEC bioanalysis to prevent cell damage or denaturation. WS_2 nanosheets exhibited low cytotoxicity and harvested red light to produce photoinduced electrons injected into the ITO electrode, with photogenerated holes and scavenged by AA. The AuNPs assembly on WS_2 nanosheets amplified the photocurrent by approximately 31 times due to the localized surface plasmon resonance (LSPR) effect of the AuNPs. The direct transfer of hot electrons from the plasmonic metal to the CB of the WS_2 nanosheet occurred by the induction of a collective oscillation of free electrons on the surface of the AuNPs under 630-nm irradiation (Table 2). A MUC1 aptamer immobilized to the nanostructured interface was used to capture MCF-7 cells as a model analyte specifically. Detection of MCF-7 cells was related to the decrease in photocurrent under irradiation with red light at a fixed voltage in amperometry at 0.1 V, showing a high linearity in a range of 10^2 – 5×10^6 cells/mL ($R^2 = 0.996$), with a LOD 21 cells/mL. The efficiency of plasmon-enhanced photoelectric conversion highlighted the effectiveness of PEC methods for sensitively detecting cancer-related biomarkers without collateral damage to the analyte biomolecules.

On the other hand, the ITO/Ag_2S/AuNPs heterojunction was used under 810-nm NIR light to quantify MCF-7 cells and dynamically evaluate cell surface glycan expression after sialidase (SA) stimulation, as shown Fig. 6B and Table 2. Ag_2S QDs showed excellent PEC properties in the NIR range, and adding AuNPs created a hybrid material with enhanced photoelectric conversion efficiency. AuNPs exhibited strong LSPR, leading to significant signal amplification. The biosensing platform featured a self-assembled monolayer (SAM) of thiol on the AuNPs, facilitating the assembly of 4-mercaptophenylboronic acid (MPBA) molecules. MPBA was a biorecognition element to capture MCF-7 cells through the reaction between SA on the cell membrane and boric acid in MPBA. This specific capture decreased photocurrent proportional to the MCF-7 concentration, with a linear range of 10^2 – 10^7 cells/mL, an $R^2 = 0.992$, and a 10^2 cells/mL LOD. The LSPR effect enhanced the photoelectric conversion efficiency by increasing light scattering and promoting electron–hole pair generation in Ag_2S QDs. The platform effectively transferred plasmonic energy from AuNPs to Ag_2S QDs, improving light absorption and charge separation, which is crucial for sensitive MCF-7 detection.

The plasmon-enhanced direct electrocatalysis of gold nanostars (AuNSs) deposited on a glassy carbon (GC) substrate for PEC detection of AA is shown in Fig. 6D [176]. The electrocatalytic performance of the AuNSs/GC system increased substantially under red light irradiation. This enhancement was attributed to the collective oscillations of conduction electrons in the light-excited AuNSs, also called LSPR. The study highlights the tunability of the LSPR of plasmonic nanostructures through parameters such as size, shape, interparticle distance, and surrounding medium properties. LSPR excitation drove electrons from the sharp tips (hot spots) of the AuNSs to higher energy levels, generating hot electrons. The anisotropic AuNSs hosted numerous "hot spots," facilitating the efficient generation of hot carriers and a reduced activation energy barrier. Likewise, the photothermal effect of LSPR excitation further increased the electrocatalytic performance of the AuNSs. The measurement at open circuit potential (OCP) led the hot electrons to the external circuit, separating them from the holes and preventing recombination. The accumulation of hot holes on the surface of AuNSs enhanced the oxidation ability toward AA, reducing the overpotential and activation energy for AA electrocatalysis in a linear range of 0.1 – 11 mM with a LOD of 10 μM and a detection sensitivity of 190.9 μA/cm^2mM. The detailed description of plasmon-mediated electrocatalysis under NIR and red-light irradiation lays the foundation for the design of PEC (bio)sensors based on anisotropic plasmonic nanostructures.

Similarly, other studies have reported the use of the conjunction between AuNPs and TMC, QDs, carbon nitrides, or metallic oxides, activated with red or NIR radiation for the detection of various targets shown in Table 2: MCF-7 cells at 808 nm [177], MC-LR cells at 980 nm [180], CCRF-CEM cells at 630 nm [56], tetracycline at 760 nm [182], and dopamine at 630 nm [183]. These studies highlight the versatility of detection modalities achievable with different arrangements of photoactive nanomaterials using red and NIR radiation. Additionally, future research can focus on developing new NIR light-sensitive materials and miniaturized photoelectrodes, applying them further for in vivo and single-cell analysis due to the versatility of irradiating nanostructured surfaces based on these photoactive nanomaterial arrangements.

Lanthanide-doped up-conversion nanoparticles (UCNPs) represent another material-sensitive NIR radiation type. UCNPs convert low-energy excitation light into high-energy fluorescence emission, leveraging their exceptional chemical stability, resistance to photobleaching, low toxicity, and ability to convert NIR light into shortwave light in the UV–visible spectral range. UCNPs typically consist of a host material like $NaYF_4$ doped with lanthanide ions such as Er^{3+}, Yb^{3+}, and Tm^{3+}, which possess discrete energy levels. Upon NIR illumination, these lanthanide ions absorb low-energy photons through sequential multi-photon absorption or energy transfer processes. A common mechanism, energy transfer upconversion (ETU), involves an ion like Yb^{3+} absorbing a photon and transferring its energy to another ion like Er^{3+}, allowing the absorption of multiple low-energy photons. In a typical two-photon upconversion process, a lanthanide ion absorbs two photons sequentially, first exciting the ion from the ground to an intermediate state and then to a higher energy state. The absorbed energy is often transferred from a sensitizer ion (e.g.,

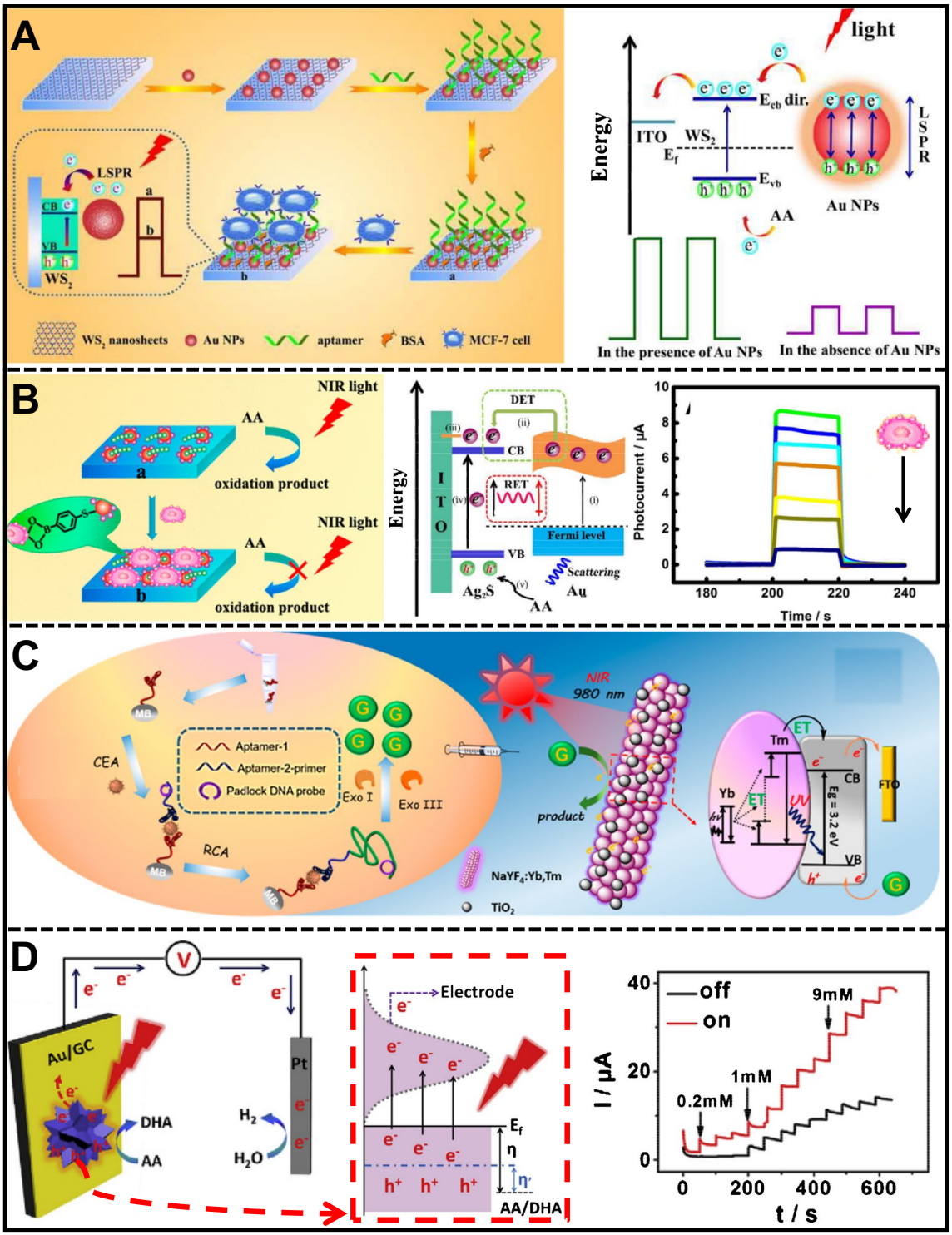

Fig. 6 **A** WS_2/AuNPs-modified platform for PEC cytosensing detection of MCF-7, reproduced with permission from Ref. [173]. **B** PEC cytosensing detection of MCF-7 based on ITO/Ag_2S/Au heterojunction, reproduced with permission from Ref. [174]. **C** FTO/$NaYF_4$:Yb,Tm@TiO_2 platform for PEC detection of CEA, reproduced with permission from Ref. [175]. **D** PEC detection of variable concentrations of AA based on GC/AuNS heterojunction, reproduced with permission from Ref. [176]

Yb^{3+}) to an activator ion (e.g., Er^{3+}), which emits a higher-energy photon. Once in the excited state, these ions can return to lower energy states by emitting photons (radiative relaxation), observed as upconversion luminescence, while minimizing non-radiative relaxation to maintain high upconversion efficiency. The application of PEC biosensors based on NIR radiation of UCNPs for detecting biomarkers in the clinical field has also been demonstrated. Tang et al. [175] presented a proof of concept of a PEC platform for the sensitive detection of carcinoembryonic antigen (CEA) under 980-nm NIR excitation, using core–shell $NaYF_4$:Yb,Tm@TiO_2 UCNPs. (Fig. 6C). The detection strategy was based on light conversion from NIR to UV and signal amplification by rolling circle amplification (RCA). The platform employed a sandwich assay with two CEA-targeting aptamers immobilized on biofunctional magnetic beads, activating RCA to produce a long guanine (G)-rich oligonucleotide strand. Enzymatic digestion released G bases by enhancing the photocurrent under NIR light excitation. This approach took advantage of the minimal photobleaching and low phototoxicity of NIR light by efficiently converting it to UV light to activate the TiO_2 layer and generate a photocurrent increase proportional to the CEA concentration. The device exhibited high sensitivity with an LOD of 3.6 pg/mL, in a linear range of 0.01–40 pg/mL ($R^2 = 0.994$), and successfully detected CEA in serum samples. This novel PEC biosensing system is promising for detecting low-abundance biomolecules in biological fluids using UCNPs.

UCNP-activated systems have been extensively used for PEC biosensing due to their ability to function as non-invasive sensitizer systems activated by 980-nm radiation, which in turn activates heterojunction systems between UCNPs and metals, metal oxides, and QDs through visible radiation emitted via fluorescence processes. The detection of alpha-fetoprotein (AFP) has been achieved through the heterojunction between $NaYF_4$:Yb,Tm/ZnO/CdS [178] and $NaYF_4$:Yb,Er@Au@CdS [186], as shown Table 2. Additionally, the detection of carcinoembryonic antigen (CEA) has been conducted using UCNP heterojunctions based on $NaYF_4$:Yb,Tm@ZnO [181], $NaYF_4$:Yb,Er/Ag_2S [165], and $NaYF_4$:Yb,Er@CdTe [185]. These studies demonstrate the versatility of such systems for analyte detection based on the conjunction of different types of materials in hybrid systems, which enhance the detection performance of PEC systems and pave the way for ongoing research into nanostructured platforms based on UCNPs.

Characterization of PEC biosensors

The accurate and rigorous characterization of PEC interfaces is crucial in developing reproducible and trustworthy detection assays. The most widely used techniques for characterizing PEC biosensing are listed in Table 3. Typically, the most relevant parameters of PEC platform surfaces are characterized in terms of surface chemistry, morphology, and (photo) electrochemical performance. Energy-dispersive X-ray spectroscopy (EDS) is a powerful analytical technique for characterizing PEC biosensors. It provides valuable information about the elemental composition, material characterization, surface modification verification, quality control, material degradation studies, and correlation with materials within the PEC system [96]. Furthermore, Fourier-transformed infrared spectroscopy (FT-IR or Raman) and X-ray photoelectron spectroscopy (XPS) are versatile analytical techniques that can be integrated into PEC biosensors to provide insights into molecular composition, chemical bonds, surface functionalization, and the monitoring of chemical changes. FT-IR and XPS enhance the understanding of PEC biosensor behavior by offering information about the chemical nature of the sensor's surface and the biomolecule-analyte interactions [187, 188].

Alternatively, ultraviolet–visible diffuse reflectance spectroscopy (UV–vis DRS) is a valuable analytical technique employed in PEC biosensors to investigate the optical properties of materials, specifically their absorption and reflectance of ultraviolet and visible light. This technique is essential for band-gap determination, quantification of photogenerated carriers, monitoring chemical changes, studying the kinetics of PEC reactions, and characterizing the performance of functionalized surfaces [189]. Finally, photoluminescence (PL) can be utilized in PEC biosensors to investigate the emission of light, usually fluorescence, from materials exposed to photons, typically from a light source. PL is commonly used for characterizing fluorescent labels, enhancing sensitivity, monitoring redox reactions, conducting kinetic studies, enabling multiplexed detection, and facilitating real-time monitoring of PEC surfaces [190].

Scanning electron microscopy (SEM), field emission scanning electron microscopy (FESEM) [191], and atomic force microscopy (AFM) [117] are powerful surface analytical techniques that can be used in PEC biosensors to study the surface morphology, structure, and composition of materials. Together, they provide comprehensive analyses of morphology, nanostructuring, chemical composition, real-time monitoring, and interaction analysis during the immobilization of biomolecules. Electrochemical techniques, including cyclic voltammetry (CV), electrochemical impedance spectroscopy (EIS), and chronoamperometry, play crucial roles in developing and characterizing PEC biosensors. CV is relevant for determining redox properties, measuring band-gaps and energy levels, kinetic studies, and assessing sensitivity in PEC devices [192]. On the other hand, EIS is used to characterize interfacial properties, monitor charge transfer resistance, and understand charge transfer rates and diffusion processes [193]. Finally, chronoamperometry is commonly used for real-time monitoring and steady-state current measurements [194].

The surface chemistry, morphology, and structural properties of nanostructured materials that alter the interfaces in PEC

Table 3 Characterization techniques of PEC biosensing interfaces

Properties	Characterization technique	Use in PEC systems	Ref
Surface chemistry	EDX	Backscattered electrons in electron microscopy are employed to obtain elemental mapping of the composition of the PEC interface	[96]
	FTIR-Raman	The functional groups available for anchoring photoactive nanomaterials and biological recognition elements are characterized by measuring the different vibrational modes determined by the bonds of atoms from these groups	[187]
	XPS	XPS offers the ability to characterize the PEC interface's chemical composition accurately. It is also helpful in monitoring the biosensor assembly based on the types of bonds formed	[188]
	UV–vis DRS	This technique leads to the characterization of solid interfaces by dispersing a fraction of the incident UV–vis radiation on its surface, as seen in PEC systems with photoactive nanomaterials	[189]
	PL	The photoactivity of materials nanostructured on the PEC biosensing interface is characterized by photoluminescence (PL), which involves the spontaneous emission of light from a material under optical excitation	[190]
Morphology	SEM-FESEM	The modification of PEC interfaces with nanostructured photoactive materials can be characterized using SEM by scanning with secondary and backscattered electrons. Furthermore, FESEM with field emission can be used to attain higher resolution, improving the observation of nanoscale details	[191]
	AFM	Critical morphological properties, such as surface topography, interaction forces, mechanical properties, electrical properties, and biomolecular interactions, can be measured at PEC sensing interfaces	[117]
Electrochemistry	CV	CV can be used to investigate redox reactions in the PEC biosensor and to measure the photocurrent generated when light activates the photoactive material in the presence of the analyte. This technique measures the photocurrent response across a range of potentials, enabling the determination of redox potentials and reaction kinetics	[192]
	EIS	EIS is employed to analyze the electrical impedance of the PEC system over a range of frequencies. It can provide insights into charge transfer resistance, adsorption processes, and other electrochemical properties relevant to PEC biosensing	[193]
	Chronoamperometry	This technique involves measuring the photocurrent at a fixed potential over a specific period. By monitoring changes in photocurrent over time, chronoamperometry can provide kinetic information about the interaction between the analyte and the bioactive elements on the sensor surface	[194]

biosensors are meticulously characterized to optimize the analytical performance of these devices. Transmission electron microscopy (TEM) is a powerful technique used to investigate nanoscale structures and compositions, offering exceptional resolution and the ability to observe internal structures [195]. X-ray diffraction (XRD) is a fundamental tool in materials research and crystallography, providing detailed information about atomic arrangements in crystals, which is essential for understanding material properties at the atomic scale [196]. Dynamic light scattering (DLS) and electrophoretic light scattering (ELS) are typically employed to study size and surface charge [197] for characterizing colloidal systems.

Concluding remarks and perspectives

PEC analysis and ongoing research in photoactive materials as transduction platforms have garnered extensive attention to enhance these devices' analytical performance. It is achieved by addressing the inherent challenges of PEC detection systems, focusing on acquiring new nanomaterials, and designing novel detection strategies. For example, nanomaterials capable of facilitating energy interconversion processes with superior efficiency have boosted the ultrasensitive, reproducible, and stable detection of various bio-analytes. Optoelectronic properties of nanomaterials exhibiting semiconductor behavior, including various metal oxides, carbon nitrides, QDs, and TMCs, have been extensively exploited for this purpose. However, challenges still must be tackled fully by a broader range of excitation sources covering more portions of the visible and NIR spectral range. Therefore, detection strategies aimed at enhancing the PEC behavior of devices have shifted toward sensitizing the materials with counterparts excitable at longer wavelengths and lower energy levels. Adopting red light and NIR excitation in PEC devices may overcome the limitations of existing (bio) sensors primarily reliant on UV–vis light that restricts their potential applications, particularly in vivo, due to its shallow tissue penetration. NIR light, spanning wavelengths greater than 650 nm, enjoys minimal spectral interference, deep tissue penetration, and limited damage to biological entities.

The possibility of miniaturizing detection assays is another strength of PEC devices, enhancing electrode design versatility without compromising performance metrics like electron transport and stability. Miniaturization enables multi-analyte detection in single measurements, which is essential for POC devices that improve disease diagnosis and intervention. Leveraging patient-specific biology, physiology, and genetic precision medicine promises to revolutionize healthcare by predicting disease risks and treatment responses. In this context, transformative diagnostics incorporate smart, innovative devices and informatic approaches using big data analytics, the Internet of Things (IoT), machine learning, blockchain, artificial intelligence (AI), augmented reality, system integration, cloud and fog computing, and smartphones, offering advanced healthcare solutions through cutting-edge converging technologies. Integrating PEC devices with these advanced systems enhances their capability to deliver precise and rapid multi-analyte detection in real-time, which is crucial for effectively implementing precision medicine. However, most research involving PEC devices for biosensing assays employs spectral ranges in the tail of the UV region, the near-UV–visible region, or a combination of the entire visible region, overlooking the significant advantages of red light and the NIR range. Integrating these underutilized spectral ranges could further enhance the sensitivity and effectiveness of PEC devices in advanced smart diagnostic applications.

The advantages of using metal oxides and carbon nitrides in photoelectrochemical biosensors are substantial. As described by conventional band theory, metal oxides offer wide-space ionic structures with minimal curvatures in their electronic bands, resulting in smaller effective masses and enhanced carrier mobility. Conversely, carbon nitrides provide an adjustable band-gap for tunable electrical conductivity, light response, and high transparency across a broad spectrum of wavelengths, making them ideal for PEC detection devices. These properties make metal oxides and carbon nitrides valuable in advancing PEC biosensors, enhancing their performance, and expanding their applications in various fields. Their high carrier charge mobility holds promise for high-speed electronic devices like thin film transistors and photovoltaic devices. Furthermore, their photoluminescent properties facilitate light emission upon electromagnetic radiation excitation, proving useful in (bio)sensors and lighting devices. Their high mechanical strength makes them ideal for optical and electronic devices requiring robust and durable materials.

Semiconductor QDs activated by UV radiation offer optoelectronic properties such as tunable size, high photoluminescence quantum yield, quantum confinement effect, and strong absorption coefficients. Their high excitation efficiency enables effective absorption and conversion of UV light into visible emission, making them ideal for light-emitting devices. The adjustable emission spectrum of QDs, achieved by varying their size, is valuable for biosensors, displays, and as marks of biomolecules. Their stability and durability ensure consistent performance over time under various conditions, and their compatibility with flexible substrates allows for use in flexible electronic and optoelectronic devices like wearable displays and (bio) sensors. TMCs with high excitation efficiency also convert UV light into visible light, which is helpful for light emission devices. Their wide adjustable band-gap range enhances versatility, and their stability and good light dispersion improve the uniformity and quality of emitted light in lighting and display applications.

Exploiting the benefits of PEC systems activated at wavelengths exceeding 650 nm is worth mentioning. Their profound tissue penetration, cellular safety, and detector stability capabilities enable the detection of biomolecules within dense samples, including tissues and bodily fluids, rendering them promising for biomedical and diagnostic applications. Additionally, they effectively mitigate autofluorescence, thereby increasing sensitivity and selectivity by minimizing interference from biological components. Moreover, these systems inflict minimal damage to cells and tissues, facilitating real-time measurements under physiological conditions without adverse effects. For example, notable optoelectronic properties of plasmonic nanoparticles enhance light capture and conversion efficiency through plasmonic coupling, thereby increasing detection sensitivity and enabling the detection of biomolecules at low concentrations. Energy UCNPs can convert infrared light into visible or ultraviolet light, allowing biosensors to be excited with shorter wavelengths and enhancing detection efficiency by reducing the autofluorescence of biological components. NIR-activated QD, which absorbs NIR light and emits visible light, is helpful for exciting PEC biosensors, thereby improving the sensitivity and selectivity of biomolecule detection. Photonic crystals manipulate and control light propagation at specific wavelengths, improving light capture efficiency and detection sensitivity.

Furthermore, PEC systems feature photodetectors characterized by enhanced stability, ensuring precise and reproducible measurements over extended periods. Their integration with biosensing approaches, such as optical coherence tomography and in vivo fluorescence imaging, paves the way for further positioning these devices into imaging systems tailored for biomedical applications. These technologies promise to develop more sensitive, selective, and efficient PEC biosensors for biomedical, food safety, and environmental applications, thus revolutionizing clinical diagnostics, pathogen detection, and environmental monitoring, ultimately improving society's health and well-being.

Acknowledgements We thank The Ruta N complex and EPM for hosting the Max Planck Tandem Groups.

Author contribution Yeison Monsalve: conceptualization, data curation, formal analysis, visualization, writing—original draft. Andrés F. Cruz-Pacheco: conceptualization, data curation, formal analysis, visualization, writing—review and editing. Jahir Orozco: conceptualization, data curation, formal analysis, funding acquisition, project administration, writing—review and editing.

Funding Open Access funding provided by Colombia Consortium. Financial support was received from the Minciencias for funding the project Validation of a Nanobiosensor to detect SARS-CoV-2 rapidly (Cod. 111593092980), the University of Antioquia, and the Max Planck Society through the Cooperation Agreement 566–1, 2014.

Availability of data and materials No datasets were generated or analyzed during the current study. Data will be made available on request.

Declarations

Ethical approval Not applicable.

Competing interests The authors declare no competing interests.

References

1. Tu W, Wang Z, Dai Z (2018) Selective photoelectrochemical architectures for biosensing: design, mechanism and responsibility. TrAC - Trends Anal Chem 105:470–483. https://doi.org/10.1016/j.trac.2018.06.007
2. Quinchia J, Echeverri D, Cruz-Pacheco AF et al (2020) Electrochemical biosensors for determination of colorectal tumor biomarkers. Micromachines 11:1–46. https://doi.org/10.3390/MI11040411
3. Huang X, Zhu Y, Kianfar E (2021) Nano biosensors: properties, applications and electrochemical techniques. J Mater Res Technol 12:1649–1672. https://doi.org/10.1016/j.jmrt.2021.03.048
4. Malik P, Katyal V, Malik V et al (2013) Nanobiosensors : concepts and variations. Int Sch Res Not 2013. https://doi.org/10.1155/2013/327435
5. Shu J, Tang D (2020) Recent advances in photoelectrochemical sensing: from engineered photoactive materials to sensing devices and detection modes. Anal Chem 92:363–377. https://doi.org/10.1021/acs.analchem.9b04199
6. Orozco J, Jiménez-Jorquera C, Fernández-Sánchez C (2009) Gold nanoparticle-modified ultramicroelectrode arrays for biosensing: a comparative assessment. Bioelectrochemistry 75:176–181. https://doi.org/10.1016/j.bioelechem.2009.03.013
7. Vásquez V, Orozco J (2023) Detection of COVID-19-related biomarkers by electrochemical biosensors and potential for diagnosis, prognosis, and prediction of the course of the disease in the context of personalized medicine. Anal Bioanal Chem 415:1003–1031. https://doi.org/10.1007/s00216-022-04237-7
8. Alzate D, Cajigas S, Robledo S et al (2020) Genosensors for differential detection of Zika virus. Talanta 210:120648. https://doi.org/10.1016/j.talanta.2019.120648
9. Vásquez G, Rey A, Rivera C et al (2017) Amperometric biosensor based on a single antibody of dual function for rapid detection of Streptococcus agalactiae. Biosens Bioelectron 87:453–458. https://doi.org/10.1016/j.bios.2016.08.082
10. Saha S, Victorious A, Pandey R et al (2020) Differential photoelectrochemical biosensing using DNA nanospacers to modulate electron transfer between metal and semiconductor nanoparticles. ACS Appl Mater Interfaces 12:36895–36905. https://doi.org/10.1021/acsami.0c09443
11. Zang Y, Fan J, Ju Y et al (2018) Current advances in semiconductor nanomaterial-based photoelectrochemical biosensing. Chem - A Eur J 24:14010–14027. https://doi.org/10.1002/chem.201801358
12. Orozco J (2023) Nanoscience, nanotechnology, and disruptive technologies in the context of precision medicine. Rev la Acad Colomb Ciencias Exactas, Fis y Nat 47:221–241. https://doi.org/10.18257/raccefyn.1895
13. Echeverri D, Calucho E, Marrugo-Ramírez J et al (2024) Capacitive immunosensing at gold nanoparticle-decorated reduced graphene oxide electrodes fabricated by one-step laser nanostructuration. Biosens Bioelectron 252. https://doi.org/10.1016/j.bios.2024.116142
14. Cruz-Pacheco AF, Echeverri D, Orozco J (2024) Role of electrochemical nanobiosensors in colorectal cancer precision medicine. TrAC - Trends Anal Chem 170. https://doi.org/10.1016/j.trac.2023.117467
15. Costa-Rama E, Teresa Fernández-Abedul M (2021) Paper-based screen-printed electrodes: a new generation of low-cost electroanalytical platforms †. https://doi.org/10.3390/bios11020051
16. Zhu C, Yang G, Li H et al (2015) Electrochemical sensors and biosensors based on nanomaterials and nanostructures. Anal Chem 87:230–249. https://doi.org/10.1021/ac5039863
17. Zhang Y, Villarreal E, Li GG et al (2020) Plasmonic nanozymes: engineered gold nanoparticles exhibit tunable plasmon-enhanced peroxidase-mimicking activity. J Phys Chem Lett 11:9321–9328. https://doi.org/10.1021/acs.jpclett.0c02640
18. Miao P, Zhou Y, Li C et al (2023) Near-infrared light-induced photoelectrochemical biosensor based on plasmon-enhanced upconversion nanocomposites for microRNA-155 detection with cascade amplifications. Biosens Bioelectron 226. https://doi.org/10.1016/j.bios.2023.115145
19. Ruggiero E, Alonso-De Castro S, Habtemariam A, Salassa L (2016) Upconverting nanoparticles for the near infrared photoactivation of transition metal complexes: new opportunities and challenges in medicinal inorganic photochemistry. Dalt Trans 45:13012–13020. https://doi.org/10.1039/c6dt01428c
20. Nan L, Giráldez-Martínez J, Stefancu A et al (2023) Investigating plasmonic catalysis kinetics on hot-spot engineered nanoantennae. Nano Lett. https://doi.org/10.1021/acs.nanolett.3c00219
21. Zhao WW, Xu JJ, Chen HY (2015) Photoelectrochemical bioanalysis: the state of the art. Chem Soc Rev 44:729–741. https://doi.org/10.1039/c4cs00228h
22. Liu S, Li C, Cheng J, Zhou Y (2006) Selective photoelectrochemical detection of DNA with high-affinity metallointercalator and tin oxide nanoparticle electrode. Anal Chem 78:4722–4726. https://doi.org/10.1021/ac052022f
23. Dong D, Zheng D, Wang FQ et al (2004) Quantitative photoelectrochemical detection of biological affinity reaction: biotin-avidin interaction. Anal Chem 76:499–501. https://doi.org/10.1021/ac035184p

24. Zhang X, Zhao Y, Li S, Zhang S (2010) Photoelectrochemical biosensor for detection of adenosine triphosphate in the extracts of cancer cells. Chem Commun 46:9173–9175. https://doi.org/10.1039/c0cc03595e
25. Tan Y, Wang Y, Li M et al (2017) Enhanced photoelectrochemical immunosensing of cardiac troponin I based on energy transfer between N-acetyl-L-cysteine capped CdAgTe quantum dots and dodecahedral Au nanoparticles. Biosens Bioelectron 91:741–746. https://doi.org/10.1016/j.bios.2017.01.040
26. Long YT, Kong C, Li DW et al (2011) Ultrasensitive determination of cysteine based on the photocurrent of nafion-functionalized CdS-MV quantum dots on an ITO electrode. Small 7:1624–1628. https://doi.org/10.1002/smll.201100427
27. Wang H, Qi C, He W et al (2018) A sensitive photoelectrochemical immunoassay of N6-methyladenosine based on dual-signal amplification strategy: Ru doped in SiO2 nanosphere and carboxylated g-C3N4. Biosens Bioelectron 99:281–288. https://doi.org/10.1016/j.bios.2017.07.042
28. Li C, Wang H, Shen J, Tang B (2015) Cyclometalated iridium complex-based label-free photoelectrochemical biosensor for dna detection by hybridization chain reaction amplification. Anal Chem 87:4283–4291. https://doi.org/10.1021/ac5047032
29. Qiu Z, Tang D (2020) Nanostructure-based photoelectrochemical sensing platforms for biomedical applications. J Mater Chem B 8:2541–2561. https://doi.org/10.1039/c9tb02844g
30. Zhang K, Lv S, Lin Z et al (2018) Bio-bar-code-based photoelectrochemical immunoassay for sensitive detection of prostate-specific antigen using rolling circle amplification and enzymatic biocatalytic precipitation. Biosens Bioelectron 101:159–166. https://doi.org/10.1016/j.bios.2017.10.031
31. Roy P, Berger S, Schmuki P (2011) TiO2 nanotubes: synthesis and applications. Angew Chemie - Int Ed 50:2904–2939. https://doi.org/10.1002/anie.201001374
32. Lin Y, Yuan G, Liu R et al (2011) Semiconductor nanostructure-based photoelectrochemical water splitting: a brief review. Chem Phys Lett 507:209–215. https://doi.org/10.1016/j.cplett.2011.03.074
33. Low J, Yu J, Jaroniec M et al (2017) Heterojunction photocatalysts. Adv Mater 29. https://doi.org/10.1002/adma.201601694
34. Wang W, Xiao J, Feng Y et al (2013) Characteristics of an air source heat pump with novel photoelectric sensors during periodic frost-defrost cycles. Appl Therm Eng 50:177–186. https://doi.org/10.1016/j.applthermaleng.2012.06.019
35. Chen PC, Periasamy AP, Harroun SG et al (2016) Photoluminescence sensing systems based on copper, gold and silver nanomaterials. Coord Chem Rev 320–321:129–138. https://doi.org/10.1016/j.ccr.2015.12.002
36. Wang Y, Wang HL, Li HY et al (2019) Enhanced high-resolution triboelectrification-induced electroluminescence for self-powered visualized interactive sensing. ACS Appl Mater Interfaces 11:13796–13802. https://doi.org/10.1021/acsami.9b02313
37. Babamiri B, Bahari D, Salimi A (2019) Highly sensitive bioaffinity electrochemiluminescence sensors: recent advances and future directions. Biosens Bioelectron 142:111530. https://doi.org/10.1016/j.bios.2019.111530
38. Xu D, Wang Y, Xiong B, Li T (2017) MEMS-based thermoelectric infrared sensors: a review. Front Mech Eng 12:557–566. https://doi.org/10.1007/s11465-017-0441-2
39. Wang Z, Yan Z, Wang F et al (2017) Highly sensitive photoelectrochemical biosensor for kinase activity detection and inhibition based on the surface defect recognition and multiple signal amplification of metal-organic frameworks. Biosens Bioelectron 97:107–114. https://doi.org/10.1016/j.bios.2017.05.011
40. Al-Hetlani E, Amin MO, Madkour M (2017) Detachable photocatalysts of anatase TiO 2 nanoparticles: annulling surface charge for immediate photocatalyst separation. Appl Surf Sci 411:355–362. https://doi.org/10.1016/j.apsusc.2017.03.151
41. Tang R, Yin R, Zhou S et al (2017) Layered MoS2 coupled MOFs-derived dual-phase TiO2 for enhanced photoelectrochemical performance. J Mater Chem A 5:4962–4971. https://doi.org/10.1039/c6ta10511d
42. Yu S, Zhang L, Zhu L et al (2019) Bismuth-containing semiconductors for photoelectrochemical sensing and biosensing. Coord Chem Rev 393:9–20. https://doi.org/10.1016/j.ccr.2019.05.008
43. Zhou Y, Yin H, Zhao W et al (2020) Electrochemical, electrochemiluminescent and photoelectrochemical bioanalysis of epigenetic modifiers : a comprehensive review. Coord Chem Rev. https://doi.org/10.1016/j.ccr.2020.213519
44. Zhao WW, Xu JJ, Chen HY (2014) Photoelectrochemical DNA biosensors. Chem Rev 114:7421–7441. https://doi.org/10.1021/cr500100j
45. Zhao W, Xu J, Chen H (2014) Chem Soc Rev Photoelectrochemical bioanalysis : the state of the art. Chem Soc Rev. https://doi.org/10.1039/C4CS00228H
46. Svitková V, Konderíková K, Nemčeková K (2022) Photoelectrochemical aptasensors for detection of viruses. Monatshefte fur Chemie 153:963–970. https://doi.org/10.1007/s00706-022-02913-z
47. Xu YT, Yu SY, Zhu YC et al (2019) Cathodic photoelectrochemical bioanalysis. TrAC - Trends Anal Chem 114:81–88. https://doi.org/10.1016/j.trac.2019.03.002
48. Wang B, Cao JT, Liu YM (2020) Recent progress of heterostructure-based photoelectrodes in photoelectrochemical biosensing: a mini review. Analyst 145:1121–1128. https://doi.org/10.1039/c9an02448d
49. Sivula K, Van De Krol R (2016) Semiconducting materials for photoelectrochemical energy conversion. Nat Rev Mater 1. https://doi.org/10.1038/natrevmats.2015.10
50. Wang J, Liu Z (2020) Recent advances in two-dimensional layered materials for photoelectrochemical sensing. TrAC - Trends Anal Chem 133:116089. https://doi.org/10.1016/j.trac.2020.116089
51. Hu T, Zheng YN, Li MJ et al (2018) A highly sensitive photoelectrochemical assay with donor-acceptor-type material as photoactive material and polyaniline as signal enhancer. Anal Chem 90:6096–6101. https://doi.org/10.1021/acs.analchem.8b00093
52. Zheng YN, Bin LW, Xiong CY et al (2016) Self-enhanced ultrasensitive photoelectrochemical biosensor based on nanocapsule packaging both donor-acceptor-type photoactive material and its sensitizer. Anal Chem 88:8698–8705. https://doi.org/10.1021/acs.analchem.6b01984
53. Wu H, Tan HL, Toe CY et al (2020) Photocatalytic and photoelectrochemical systems: similarities and differences. Adv Mater 32:1–21. https://doi.org/10.1002/adma.201904717
54. Divyapriya G, Singh S, Martínez-Huitle CA et al (2021) Treatment of real wastewater by photoelectrochemical methods: an overview. Chemosphere 276:130188. https://doi.org/10.1016/j.chemosphere.2021.130188
55. Emeline AV, Kuznetsov VN, Ryabchuk VK, Serpone N (2012) On the way to the creation of next generation photoactive materials. Environ Sci Pollut Res 19:3666–3675. https://doi.org/10.1007/s11356-011-0665-3
56. Li J, Lin X, Zhang Z et al (2019) Red light-driven photoelectrochemical biosensing for ultrasensitive and scatheless assay of tumor cells based on hypotoxic AgInS 2 nanoparticles. Biosens Bioelectron 126:332–338. https://doi.org/10.1016/j.bios.2018.09.096
57. Mesquita MQ, Dias CJ, Neves MGPMS et al (2018) Revisiting current photoactive materials for antimicrobial photodynamic therapy. Molecules 23. https://doi.org/10.3390/molecules23102424

58. Zhou Y, Yin H, Ai S (2021) Applications of two-dimensional layered nanomaterials in photoelectrochemical sensors: a comprehensive review. Coord Chem Rev 447:214156. https://doi.org/10.1016/j.ccr.2021.214156
59. Rodríguez-Seco C, Wang YS, Zaghib K, Ma D (2022) Photoactive nanomaterials enabled integrated photo-rechargeable batteries. Nanophotonics 11(8):1443–1484
60. Jain R, Mohanty S, Sarode I et al (2023) Multifunctional photoactive nanomaterials for photodynamic therapy against tumor: recent advancements and perspectives. Pharmaceutics 15:1–22. https://doi.org/10.3390/pharmaceutics15010109
61. Liang S, Pierce DT, Amiot C, Zhao X (2005) Photoactive nanomaterials for sensing trace analytes in biological samples. Synth React Inorganic, Met Nano-Metal Chem 35:661–668. https://doi.org/10.1080/15533170500299859
62. Choi SK (2016) Mechanistic basis of light induced cytotoxicity of photoactive nanomaterials. NanoImpact 3–4:81–89. https://doi.org/10.1016/j.impact.2016.09.001
63. Louie SM, Tilton RD, Lowry GV (2016) Critical review: impacts of macromolecular coatings on critical physicochemical processes controlling environmental fate of nanomaterials. Environ Sci Nano 3:283–310. https://doi.org/10.1039/c5en00104h
64. Li J, Zhang JZ (2009) Optical properties and applications of hybrid semiconductor nanomaterials. Coord Chem Rev 253:3015–3041. https://doi.org/10.1016/j.ccr.2009.07.017
65. Yao B, Zhang J, Fan X et al (2019) Surface engineering of nanomaterials for photo-electrochemical water splitting. Small 15:1–20. https://doi.org/10.1002/smll.201803746
66. Mishra NS, Saravanan P (2018) A review on the synergistic features of hexagonal boron nitride (white graphene) as adsorbent-photo active nanomaterial. ChemistrySelect 3:8023–8034. https://doi.org/10.1002/slct.201801524
67. Lei Z, Ling X, Mei Q et al (2020) An excitation navigating energy migration of lanthanide ions in upconversion nanoparticles. Adv Mater 32:1–7. https://doi.org/10.1002/adma.201906225
68. Juay J, Yang JCE, Bai H, Sun DD (2022) Novel ultralong and photoactive Bi2Ti4O11/TiO2 heterojunction nanofibers toward efficient textile wastewater treatment. RSC Adv 12:25449–25456. https://doi.org/10.1039/d2ra02181a
69. Edvinsson T (2018) Optical quantum confinement and photocatalytic properties in two-, one- and zerodimensional nanostructures. R Soc Open Sci 5. https://doi.org/10.1098/rsos.180387
70. Ma X, Kang J, Wu Y et al (2022) Recent advances in metal/covalent organic framework-based materials for photoelectrochemical sensing applications. TrAC - Trends Anal Chem 157:116793. https://doi.org/10.1016/j.trac.2022.116793
71. Zhao W, Xu J, Chen H (2017) Biosensors and bioelectronics photoelectrochemical enzymatic biosensors. Biosens Bioelectron 92:294–304. https://doi.org/10.1016/j.bios.2016.11.009
72. Zhao WW, Xu JJ, Chen HY (2017) Photoelectrochemical enzymatic biosensors. Biosens Bioelectron 92:294–304. https://doi.org/10.1016/j.bios.2016.11.009
73. Lyu L, Cheong H, Ai X et al (2018) Near-infrared light-mediated rare-earth nanocrystals: recent advances in improving photon conversion and alleviating the thermal effect. NPG Asia Mater 10:685–702. https://doi.org/10.1038/s41427-018-0065-y
74. Vitiello G, Luciani G (2021) Photocatalysis: activity of nanomaterials. Catalysts 11:10–12. https://doi.org/10.3390/catal11050611
75. Monllor-Satoca D, Díez-García MI, Lana-Villarreal T, Gómez R (2020) Photoelectrocatalytic production of solar fuels with semiconductor oxides: materials, activity and modeling. Chem Commun 56:12272–12289. https://doi.org/10.1039/d0cc04387g
76. Du T, Adeleye AS, Zhang T et al (2018) Influence of light wavelength on the photoactivity, physicochemical transformation, and fate of graphene oxide in aqueous media. Environ Sci Nano 5:2590–2603. https://doi.org/10.1039/C8EN00593A
77. Chang JS, Chong MN (2021) Photoactive nanomaterials: applications in wastewater treatment and their environmental fate. Heterog Photocatal 331–349. https://doi.org/10.1002/9783527815296.ch14
78. Bilge S (2023) Trends in analytical chemistry current trends and strategies in the development of green MXene- based photoelectrochemical sensing application. Trends Anal Chem 163. https://doi.org/10.1016/j.trac.2023.117059
79. Qiu Z, Tang D (2020) Nanostructures-based photoelectrochemical sensing platforms for biomedical applications. J Mater Chem B. https://doi.org/10.1039/C9TB02844G
80. Zhao W, Xu J, Chen H (2016) Photoelectrochemical aptasensing. Trends Anal Chem. https://doi.org/10.1016/j.trac.2016.06.020
81. Ge L, Liu Q, Kun W (2019) Recent developments of photoelectrochemical biosensors for food analysis. J Mater Chem B 7283–7300. https://doi.org/10.1039/c9tb01644a
82. Kang Z, Gu Y, Yan X et al (2015) Enhanced photoelectrochemical property of ZnO nanorods array synthesized on reduced graphene oxide for self-powered biosensing application. Biosens Bioelectron 64:499–504. https://doi.org/10.1016/j.bios.2014.09.055
83. Wang H, Wang Y, Zhang Y et al (2016) Photoelectrochemical immunosensor for detection of carcinoembryonic antigen based on 2D TiO 2 nanosheets and carboxylated graphitic carbon nitride. Nat Publ Gr 1–7. https://doi.org/10.1038/srep27385
84. Li Y, Zhang X, Liu X, Pan W (2021) Chemical science immunomodulators for cancer immunotherapy. R Soc Chem 3130–3145. https://doi.org/10.1039/d0sc06557a
85. Zhang X, Li S, Jin X, Li X (2011) Biosensors and bioelectronics aptamer based photoelectrochemical cytosensor with layer-by-layer assembly of CdSe semiconductor nanoparticles as photoelectrochemically active species. Biosens Bioelectron 26:3674–3678. https://doi.org/10.1016/j.bios.2011.01.030
86. Liu F, Zhang Y, Yu J et al (2014) Biosensors and bioelectronics application of ZnO / graphene and S6 aptamers for sensitive photoelectrochemical detection of SK-BR-3 breast cancer cells based on a disposable indium tin oxide device. Biosens Bioelectron 51:413–420. https://doi.org/10.1016/j.bios.2013.07.066
87. Zhang X, Liu M, Liu H, Zhang S (2014) Biosensors and bioelectronics low-toxic Ag 2 S quantum dots for photoelectrochemical detection glucose and cancer cells. Biosens Bioelectron 56:307–312. https://doi.org/10.1016/j.bios.2014.01.033
88. Ruan Y, Xu F, Zhao W et al (2016) Protein binding bends the gold nanoparticle capped DNA sequence : towards novel energy-transfer based photoelectrochemical protein detection. Anal Chem. https://doi.org/10.1021/acs.analchem.6b00012
89. Xiao X, Zheng S, Li X, Zhang G, Xiaotian X, Xue H, Pang H (2017) Facile synthesis of ultrathin Ni-MOF nanobelts for high-efficiency determination of glucose in human serum. Mater Chem B. https://doi.org/10.1039/C7TB00180K
90. Hong-Lei Shuai X-JH (2017) Molybdenum disulfide spheres-based Electrochemical aptasensor for proteins detection. Mater Chem B. https://doi.org/10.1039/C7TB01276D
91. Yang Y, Liang J, Jin W et al (2020) The design and growth of peanut-like CuS/BiVO4 composites for photoelectrochemical sensing. RSC Adv 14670–14678. https://doi.org/10.1039/d0ra01307b
92. Pang Y, Xu G, Feng Q et al (2017) Synthesis of # -Bi2Mo3O12 / TiO2 nanotube arrays for photoelectrochemical COD detection application synthesis of α - Bi 2 Mo 3 O 12 / TiO 2 Nanotube arrays for photoelectrochemical COD. Langmuir. https://doi.org/10.1021/acs.langmuir.7b01826
93. Wang Z, Yu R, Zeng H et al (2019) Nucleic acid-based ratiometric electrochemiluminescent, electrochemical and photoelectrochemical biosensors: a review. Mikrochim Acta 186(7):405
94. Dai H, Zhang S, Hong Z, Lin Y (2016) A potentiometric addressable photoelectrochemical biosensor for sensitive detection of

two biomarkers. Anal Chem 88:9532–9538. https://doi.org/10.1021/acs.analchem.6b02101
95. Yang L, Zhang S, Liu X (2020) Detection signal amplification strategies at nanomaterial-based photoelectrochemical biosensors. J Mater Chem B. https://doi.org/10.1039/d0tb01191f
96. Mo F, Wu J, Chen M et al (2019) Enzyme-free "on-off-on" photoelectrochemical biosensor based on cascaded quadratic amplification strategy for miRNA 141 detection. Sensors Actuators, B Chem 289:269–276. https://doi.org/10.1016/j.snb.2019.03.044
97. Xue M (2021) Applications of nanomaterials-based photoelectrochemical biosensors for highly sensitive detection. 2021 3rd Int Acad Exch Conf Sci Technol Innov IAECST 2021 1037–1041. https://doi.org/10.1109/IAECST54258.2021.9695631
98. Heydari-Bafrooei E, Ensafi AA (2023) Nanomaterials-based biosensing strategies for biomarkers diagnosis, a review. Biosens Bioelectron X 13:100245. https://doi.org/10.1016/j.biosx.2022.100245
99. Kang Z, Yan X, Wang Y et al (2016) Self-powered photoelectrochemical biosensing platform based on Au NPs@ZnO nanorods array. Nano Res 9:344–352. https://doi.org/10.1007/s12274-015-0913-9
100. Huang Q, Wang Y, Lei L et al (2016) Photoelectrochemical biosensor for acetylcholinesterase activity study based on metal oxide semiconductor nanocomposites. J Electroanal Chem 781:377–382. https://doi.org/10.1016/j.jelechem.2016.07.007
101. Shu J, Qiu Z, Lv S et al (2018) Plasmonic enhancement coupling with defect-engineered TiO2-x: a mode for sensitive photoelectrochemical biosensing. Anal Chem 90:2425–2429. https://doi.org/10.1021/acs.analchem.7b05296
102. Okoth OK, Yan K, Feng J, Zhang J (2018) Label-free photoelectrochemical aptasensing of diclofenac based on gold nanoparticles and graphene-doped CdS. Sensors Actuators, B Chem 256:334–341. https://doi.org/10.1016/j.snb.2017.10.089
103. Bellani S, Ghadirzadeh A, Meda L et al (2015) Hybrid organic/inorganic nanostructures for highly sensitive photoelectrochemical detection of dissolved oxygen in aqueous media. Adv Funct Mater 25:4531–4538. https://doi.org/10.1002/adfm.201500701
104. Chen Y, Wang Y, Yan P et al (2020) Co3O4 nanoparticles/graphitic carbon nitride heterojunction for photoelectrochemical aptasensor of oxytetracycline. Anal Chim Acta 1125:299–307. https://doi.org/10.1016/j.aca.2020.05.038
105. Tang L, Ouyang X, Peng B et al (2019) Highly sensitive detection of microcystin-LR under visible light using a self-powered photoelectrochemical aptasensor based on a CoO/Au/g-C3N4 Z-scheme heterojunction. Nanoscale 11:12198–12209. https://doi.org/10.1039/c9nr03004b
106. Li Y, Bu Y, Jiang F et al (2020) Fabrication of ultra-sensitive photoelectrochemical aptamer biosensor: based on semiconductor/DNA interfacial multifunctional reconciliation via 2D–C3N4. Biosens Bioelectron 150:111903. https://doi.org/10.1016/j.bios.2019.111903
107. Qi H, Sun B, Dong J et al (2019) Facile synthesis of two-dimensional tailored graphitic carbon nitride with enhanced photoelectrochemical properties through a three-step polycondensation method for photocatalysis and photoelectrochemical immunosensor. Sensors Actuators, B Chem 285:42–48. https://doi.org/10.1016/j.snb.2019.01.028
108. Li X, Zhu L, Zhou Y et al (2017) Enhanced photoelectrochemical method for sensitive detection of protein kinase A activity using TiO2/g-C3N4, PAMAM dendrimer, and alkaline phosphatase. Anal Chem 89:2369–2376. https://doi.org/10.1021/acs.analchem.6b04184
109. Dong YX, Cao JT, Wang B et al (2018) Spatial-resolved photoelectrochemical biosensing array based on a CdS@g-C3N4 heterojunction: a universal immunosensing platform for accurate detection. ACS Appl Mater Interfaces 10:3723–3731. https://doi.org/10.1021/acsami.7b13557
110. Dong YX, Cao JT, Wang B et al (2017) Exciton-plasmon interactions between CdS@g-C3N4 heterojunction and Au@Ag nanoparticles coupled with DNAase-triggered signal amplification: toward highly sensitive photoelectrochemical bioanalysis of microRNA. ACS Sustain Chem Eng 5:10840–10848. https://doi.org/10.1021/acssuschemeng.7b02774
111. Sun M, Li R, Zhang J et al (2019) One-pot synthesis of a CdS-reduced graphene oxide-carbon nitride composite for self-powered photoelectrochemical aptasensing of PCB72. Nanoscale 11:5982–5988. https://doi.org/10.1039/C9NR00966C
112. Wang F, Liu Y, Zhang L et al (2022) Photoelectrochemical biosensor based on CdS quantum dots anchored h-BN nanosheets and tripodal DNA walker for sensitive detection of miRNA-141. Anal Chim Acta 1226:340265. https://doi.org/10.1016/j.aca.2022.340265
113. Zang Y, Fan J, Zhang H et al (2020) Dual-functional β-CD@CdS nanorod/WS2 nanosheet heterostructures coupled with strand displacement reaction-mediated photocurrent quenching for an ultrasensitive MicroRNA-21 assay. Electrochim Acta 334:135581. https://doi.org/10.1016/j.electacta.2019.135581
114. Hun X, Wang S, Wang S et al (2017) A photoelectrochemical sensor for ultrasensitive dopamine detection based on single-layer NanoMoS 2 modified gold electrode. Sensors Actuators B Chem 249:83–89. https://doi.org/10.1016/j.snb.2017.04.065
115. Zheng Y, Cui X, Yin H et al (2023) Antibody-free photoelectrochemical biosensor for DNA carboxylation detection based on SnS2@Ti3C2 heterojunction. Anal Chim Acta 1251:341011. https://doi.org/10.1016/J.ACA.2023.341011
116. Jiang D, Du X, Zhou L et al (2017) New insights towards efficient charge separation mechanism for high-performances photoelectrochemical aptasensing : enhanced charge carriers lifetime via coupling ultrathin MoS2 nanoplates with nitrogen doped graphene quantum dots. New insights towards eff. https://doi.org/10.1021/acs.analchem.6b04949
117. Li F, Wang S, Yin H et al (2020) Photoelectrochemical biosensor for DNA formylation detection in genomic DNA of maize seedlings based on black Tio2-enhanced photoactivity of MoS2/WS2 heterojunction. ACS Sensors 5:1092–1101. https://doi.org/10.1021/acssensors.0c00036
118. Huang L, Wang C, Yang Y et al (2023) A light-driven photoelectrochemical sensor for highly selective detection of hydroquinone based on type-II heterojunction formed by carbon nanotubes immobilized in 3D honeycomb CdS/SnS2. J Colloid Interface Sci 643:585–599. https://doi.org/10.1016/j.jcis.2023.03.141
119. Xiao FX, Liu B (2018) Plasmon-dictated photo-electrochemical water splitting for solar-to-chemical energy conversion: current status and future perspectives. Adv Mater Interfaces 5:1–21. https://doi.org/10.1002/admi.201701098
120. Xia C, Wang H, Kim JK, Wang J (2021) Rational design of metal oxide-based heterostructure for efficient photocatalytic and photoelectrochemical systems. Adv Funct Mater 31:1–31. https://doi.org/10.1002/adfm.202008247
121. Wang L, Si W, Tong Y et al (2020) Graphitic carbon nitride (g-C3N4)-based nanosized heteroarrays: promising materials for photoelectrochemical water splitting. Carbon Energy 2:223–250. https://doi.org/10.1002/cey2.48
122. Zhou H, Liu J, Zhang S (2015) Quantum dot-based photoelectric conversion for biosensing applications. TrAC - Trends Anal Chem 67:56–73. https://doi.org/10.1016/j.trac.2014.12.007
123. Sumesh CK, Peter SC (2019) Two-dimensional semiconductor transition metal based chalcogenide based heterostructures for water splitting applications. Dalt Trans 48:12772–12802. https://doi.org/10.1039/c9dt01581g

124. Zhang Y, Guo W, Zhang Y, Wei WD (2021) Plasmonic photoelectrochemistry. In View of Hot Carriers 2006654:1–16. https://doi.org/10.1002/adma.202006654
125. Duchene J, Tagliabue G, Welch AJ et al (2018) Reduction with plasmonic Au / p-GaN photocathodes hot hole collection and photoelectrochemical CO 2 reduction with plasmonic Au / p-GaN photocathodes. https://doi.org/10.1021/acs.nanolett.8b00241
126. Rani KK, Devasenathipathy R, Wang J et al (2022) Electrochemistry plasmonic photoelectrochemical reactions on noble metal electrodes of nanostructures. Curr Opin Electrochem 34:100985. https://doi.org/10.1016/j.coelec.2022.100985
127. Zhang P, Wang T, Gong J (2015) Mechanistic understanding of the plasmonic enhancement for solar water splitting. Adv Mater 5328–5342. https://doi.org/10.1002/adma.201500888
128. Zhao W-W, Tian C-Y, Xu J-J, Chen H-Y (2012) The coupling of localized surface plasmon resonance-based photoelectrochemistry and nanoparticle size effect: towards novel plasmonic photoelectrochemical biosensing. Chem Comm 1:895–897. https://doi.org/10.1039/c1cc16775h
129. Zhang N, Han C, Xu Y et al (2016) Near-field dielectric scattering promotes optical absorption by platinum nanoparticles. Nat Photonics 10. https://doi.org/10.1038/nphoton.2016.76
130. Tang J, Xiong P, Cheng Y et al (2019) Biosensors and bioelectronics enzymatic oxydate-triggered AgNPs etching : a novel signal-on photoelectrochemical immunosensing platform based on Ag @ AgCl nanocubes loaded RGO plasmonic heterostructure. Biosens Bioelectron 130:125–131. https://doi.org/10.1016/j.bios.2019.01.014
131. Kochuveedu ST, Jang YH, Kim DH (2013) A study on the mechanism for the interaction of light with noble metal-metal oxide semiconductor nanostructures for various photophysical applications. Chem Soc Rev. https://doi.org/10.1039/c3cs60043b
132. Wang G, Yang Y, Ling Y, Wang H, Lu X, Pu Y-C, Zhang JZ, Tong Y, Li Y (2016) An electrochemical method to enhance the performance of metal oxides for photoelectrochemical water oxidation. Mater Chem A. https://doi.org/10.1039/C5TA10477G
133. Katz JE, Gingrich TR, Santori EA, Lewis NS (2009) Combinatorial synthesis and high-throughput photopotential and photocurrent screening of mixed-metal oxides for photoelectrochemical water splitting. Energy Environ Sci 103–112. https://doi.org/10.1039/b812177j
134. Yang Y, Niu S, Han D et al (2017) Progress in developing metal oxide nanomaterials for photoelectrochemical water splitting. Adv Energy Mater 1700555:1–26. https://doi.org/10.1002/aenm.201700555
135. Links DA (2012) Oxygen-deficient metal oxide nanostructures for photoelectrochemical water oxidation and other applications. Nanoscale 6682–6691. https://doi.org/10.1039/c2nr32222f
136. Ros C, Andreu T, Morante JR (2020) Photoelectrochemical water splitting: a road from stable metal oxides to protected thin film solar cells. Mater Chem A. https://doi.org/10.1039/D0TA02755C
137. Venkata C, Raghava K, Shetti NP et al (2019) ScienceDirect hetero-nanostructured metal oxide-based hybrid photocatalysts for enhanced photoelectrochemical water splitting: a review. Int J Hydrogen Energy 45:18331–18347. https://doi.org/10.1016/j.ijhydene.2019.02.109
138. Nadzirah S, Gopinath SCB, Parmin NA et al (2022) State-of-the-art on functional titanium dioxide-integrated nano-hybrids in electrical biosensors. Crit Rev Anal Chem 52:637–648. https://doi.org/10.1080/10408347.2020.1816447
139. Wu N (2018) Plasmonic metal-semiconductor photocatalysts and photoelectrochemical cells: a review. Nanoscale. https://doi.org/10.1039/C7NR08487K
140. Rajabpour A, Bazrafshan S, Volz S (2019) Carbon-nitride 2D nanostructures: thermal conductivity and interfacial thermal conductance with the silica substrate. Phys Chem Chem Phys 21:2507–2512. https://doi.org/10.1039/c8cp06992a
141. Ong WJ, Tan LL, Chai SP et al (2015) Surface charge modification via protonation of graphitic carbon nitride (g-C3N4) for electrostatic self-assembly construction of 2D/2D reduced graphene oxide (rGO)/g-C3N4 nanostructures toward enhanced photocatalytic reduction of carbon dioxide to methane. Nano Energy 13:757–770. https://doi.org/10.1016/j.nanoen.2015.03.014
142. Zeng H, Liu Y, Xu Z et al (2019) Construction of a Z-scheme g-C3N4/Ag/AgI heterojunction for highly selective photoelectrochemical detection of hydrogen sulfide. Chem Commun 55:11940–11943. https://doi.org/10.1039/c9cc05356e
143. Inagaki M, Tsumura T, Kinumoto T, Toyoda M (2019) Graphitic carbon nitrides (g -C 3 N 4) with comparative discussion to carbon materials. Carbon N Y 141:580–607. https://doi.org/10.1016/j.carbon.2018.09.082
144. Li W, Jiang D, Yan P et al (2019) Graphitic carbon nitride/α-Fe2O3 heterostructures for sensitive photoelectrochemical nonenzymatic glucose sensor. Inorg Chem Commun 106:211–216. https://doi.org/10.1016/j.inoche.2019.06.015
145. Low SS, Chen Z, Li Y et al (2021) Trends in analytical chemistry design principle in biosensing : critical analysis based on graphitic carbon nitride (G-C 3 N 4) photoelectrochemical biosensor. Trends Anal Chem 145:116454. https://doi.org/10.1016/j.trac.2021.116454
146. Liang J, Chen D, Yao X et al (2019) Recent progress and development in inorganic halide perovskite quantum dots for photoelectrochemical applications. Nano-Micro Small 1903398:1–20. https://doi.org/10.1002/smll.201903398
147. Shu J, Tang D (2017) Current advances in quantum-dots-based photoelectrochemical immunoassays. Chem an Asian J 2780–2789. https://doi.org/10.1002/asia.201701229
148. Yue Z, Lisdat F, Parak WJ et al (2013) Quantum-dot-based photoelectrochemical sensors for chemical and biological detection. Appl Mater Interfaces. https://doi.org/10.1021/am3028662
149. Zhang N, Zhang L, Ruan Y et al (2017) Biosensors and bioelectronics quantum-dots-based photoelectrochemical bioanalysis highlighted with recent examples. Biosens Bioelectron 94:207–218. https://doi.org/10.1016/j.bios.2017.03.011
150. Jin L, Zhao H, Wang ZM, Rosei F (2021) Quantum dots-based photoelectrochemical hydrogen evolution from water splitting. Adv Energy Mater 2003233:1–28. https://doi.org/10.1002/aenm.202003233
151. Van EM, Lorenz DB, Sambur JB (2022) Answering old questions with new techniques : understanding performance-limiting factors in transition metal dichalcogenide photoelectrochemical solar cells. Curr Opin Electrochem 37:101173. https://doi.org/10.1016/j.coelec.2022.101173
152. Bulters D, Sukanya R, Daniele C et al (2022) Review — recent developments in the applications of 2D transition metal dichalcogenides as electrocatalysts in the generation of hydrogen for renewable energy conversion review — recent developments in the applications of 2D transition metal dichalcogenid. Electrochem Soc. https://doi.org/10.1149/1945-7111/ac7172
153. Nguyen V, Nguyen TP, Le T, Vo DN (2020) Recent advances in two-dimensional transition metal dichalcogenides as photoelectrocatalyst for hydrogen evolution reaction. Soc Chem Ind 1. https://doi.org/10.1002/jctb.6335
154. Wang J, Liu Z (2020) Trends in analytical chemistry recent advances in two-dimensional layered materials for photoelectrochemical sensing. Trends Anal Chem 133:116089. https://doi.org/10.1016/j.trac.2020.116089

155. Pumera M, Loo AH (2014) Layered transition-metal dichalcogenides (MoS2 and WS2) for sensing and biosensing. Trends Anal Chem 61:49–53. https://doi.org/10.1016/j.trac.2014.05.009
156. Jiang D, Du X, Liu Q et al (2019) MoS 2 / nitrogen doped graphene hydrogels p-n heterojunction : efficient charge transfer property for highly sensitive and selective photoelectrochemical analysis of chloramphenicol. Biosens Bioelectron 126:463–469. https://doi.org/10.1016/j.bios.2018.11.018
157. Fan D, Wang H, Khan MS et al (2017) An ultrasensitive photoelectrochemical immunosensor for insulin detection based on BiOBr/Ag2S composite by in-situ growth method with high visible-light activity. Biosens Bioelectron 97:253–259. https://doi.org/10.1016/j.bios.2017.05.044
158. Ge L, Hong Q, Li H et al (2019) Direct-laser-writing of metal sulfide-graphene nanocomposite photoelectrode toward sensitive photoelectrochemical sensing. Adv Funct Mater 1904000:1–10. https://doi.org/10.1002/adfm.201904000
159. Zheng L, Teng F, Ye X et al (2019) Photo / electrochemical applications of metal sulfide / TiO 2 heterostructures. Adv Funct Mater 1902355:1–32. https://doi.org/10.1002/aenm.201902355
160. Ibrahim I, Lim HN, Abou-zied OK et al (2016) Cadmium sulfide nanoparticles decorated with Au quantum dots as ultrasensitive photoelectrochemical sensor for selective detection of copper (II) ions. J Phys Chem. https://doi.org/10.1021/acs.jpcc.6b06929
161. Shi L, Yin Y, Zhang L et al (2019) Design and engineering heterojunctions for the photoelectrochemical monitoring of environmental pollutants : a review. Appl Catal B Environ 248:405–422. https://doi.org/10.1016/j.apcatb.2019.02.044
162. Yang P, Hou X, Gao X et al (2024) Recent trends in self-powered photoelectrochemical sensors: from the perspective of signal output. ACS Sensors. https://doi.org/10.1021/acssensors.3c02198
163. Zang Y, Fan J, Yun J, Xue HG Current advances in semiconductor nanomaterials-based photoelectrochemical biosensing. Chem - A Eur J. https://doi.org/10.1002/chem.201801358
164. Li T, Dong H, Hao Y et al (2022) Near-infrared responsive photoelectrochemical biosensors. Electroanalysis 34:956–965. https://doi.org/10.1002/elan.202100355
165. Qiu Z, Shu J, Tang D (2018) NaYF4:Yb, Er Upconversion nanotransducer with in situ fabrication of Ag2S for near-infrared light responsive photoelectrochemical biosensor. Anal Chem 90:12214–12220. https://doi.org/10.1021/acs.analchem.8b03446
166. Zhai Y, Liu D, Jiang Y et al (2019) Near-infrared-light-triggered photoelectrochemical biosensor for detection of alpha-fetoprotein based on upconversion nanophosphors. Sensors Actuators, B Chem 286:468–475. https://doi.org/10.1016/j.snb.2019.01.080
167. Han Q, Zhao X, Na N, Ouyang J (2021) Integrating near-infrared visual fluorescence with a photoelectrochemical sensing system for dual readout detection of biomolecules. Anal Chem 93:3486–3492. https://doi.org/10.1021/acs.analchem.0c04802
168. Sun SK, Wang HF, Yan XP (2018) Engineering persistent luminescence nanoparticles for biological applications: from biosensing/bioimaging to theranostics. Acc Chem Res 51:1131–1143. https://doi.org/10.1021/acs.accounts.7b00619
169. Lei Z, Sun C, Pei P et al (2019) Stable, wavelength-tunable fluorescent dyes in the NIR-II region for in vivo high-contrast bioimaging and multiplexed biosensing. Angew Chemie 131:8250–8255. https://doi.org/10.1002/ange.201904182
170. Cai Y, Wei Z, Song C et al (2019) Optical nano-agents in the second near-infrared window for biomedical applications. Chem Soc Rev 48:22–37. https://doi.org/10.1039/c8cs00494c
171. Huang L, Liang Z, Zhang F, Luo H, Liang R, Han F, Wu Z, Han D, Shen J, Niu L (2022) Upconversion NaYF4:Yb/Er–TiO2–Ti3C2 heterostructure-based near-infrared light-driven photoelectrochemical biosensor for highly sensitive and selective d-Serine detection. Anal Chem. https://doi.org/10.1021/acs.analchem.2c04101
172. Tian Y, Cui Q, Xu L et al (2021) Alloyed AuPt nanoframes loaded on h-BN nanosheets as an ingenious ultrasensitive near-infrared photoelectrochemical biosensor for accurate monitoring glucose in human tears. Biosens Bioelectron 192:113490. https://doi.org/10.1016/j.bios.2021.113490
173. Li R, Yan R, Bao J, Tu W, Dai Z (2016) A localized surface plasmon resonance-enhanced photoelectrochemical biosensing strategy for highly sensitive and scatheless cell assay under red light excitation. Chem Commun. https://doi.org/10.1039/C6CC05964C
174. Li R, Tu W, Wang H, Dai Z (2018) Near-infrared light excited and localized surface plasmon resonance-enhanced photoelectrochemical biosensing platform for cell analysis. Anal Chem 90:9403–9409. https://doi.org/10.1021/acs.analchem.8b02047
175. Qiu Z, Shu J, Tang D (2018) Near-infrared-to-ultraviolet light-mediated photoelectrochemical aptasensing platform for cancer biomarker based on core-shell NaYF4:Yb, Tm@TiO2 upconversion microrods. Anal Chem 90:1021–1028. https://doi.org/10.1021/acs.analchem.7b04479
176. Wang SS, Hu WC, Liu FF et al (2019) Insights into direct plasmon-activated eletrocatalysis on gold nanostar via efficient photothermal effect and reduced activation energy. Electrochim Acta 301:359–365. https://doi.org/10.1016/j.electacta.2019.01.172
177. Xu X, Ding Z, Zhang X et al (2023) A near-infrared photoelectrochemical aptasensing system based on Bi 2 O 2 S nanoflowers and gold nanoparticles for high-performance determination of MCF-7 cells. Anal Chim Acta 1251:340982. https://doi.org/10.1016/j.aca.2023.340982
178. Zhai Y, Liu D, Jiang Y et al (2019) Near-infrared-light-triggered photoelectrochemical biosensor for detection of alpha-fetoprotein based on upconversion nanophosphors. Sensors Actuators B Chem 286:468–475. https://doi.org/10.1016/j.snb.2019.01.080
179. Zhou X, Geng H, Shi P et al (2024) NIR-driven photoelectrochemical-fluorescent dual-mode biosensor based on bipedal DNA walker for ultrasensitive detection of microRNA. Biosens Bioelectron 247:115916. https://doi.org/10.1016/j.bios.2023.115916
180. Zheng C, Yin M, Su B et al (2021) A novel near-infrared light-responsive photoelectrochemical platform for detecting microcystin-LR in fish based on Ag 2 S cubes and plasmonic Au nanoparticles. Talanta 221:121447. https://doi.org/10.1016/j.talanta.2020.121447
181. Lv S, Zhang K, Zhu L, Tang D (2020) ZIF-8-Assisted NaYF4:Yb, Tm@ZnO converter with exonuclease III- powered DNA walker for near-infrared light responsive biosensor. Anal Chem. https://doi.org/10.1021/acs.analchem.9b04710
182. Fu B, Wu W, Gan L, Zhang Z (2019) Bulk/surface defects engineered TiO 2 nanotube photonic crystals coupled with plasmonic gold nanoparticles for effective in vivo near-infrared light photoelectrochemical detection. Anal Chem. https://doi.org/10.1021/acs.analchem.9b03733
183. Ji J, Shen Y, Wu K et al (2019) Exfoliation and sensitization of 2D carbon nitride for photoelectrochemical biosensing under red light. Chem - A Eur J. https://doi.org/10.1002/chem.201904076
184. Chen X, Xu W, Jiang Y et al (2017) A novel upconversion luminescence derived photoelectrochemical immunoassay: ultrasensitive detection to alpha-fetoprotein. Nanoscale 16357–16364. https://doi.org/10.1039/c7nr05577c
185. Qiu Z, Shu J, Liu J, Tang D (2019) Dual-channel photoelectrochemical ratiometric aptasensor with up-converting nanocrystals using spatial-resolved technique on homemade 3D printed device. Anal Chem. https://doi.org/10.1021/acs.analchem.8b05455
186. Luo Z, Zhang L, Zeng R et al (2018) Near-infrared light-excited core-core-shell UCNP @ Au @ CdS upconversion nanospheres for ultrasensitive photoelectrochemical enzyme immunoassay

near-infrared light-excited core-core-shell UCNP @ Au @ CdS upconversion nanospheres for ultrasensitive photoel. Anal Chem. https://doi.org/10.1021/acs.analchem.8b02421
187. Mazzaracchio V, Marrone R, Forchetta M et al (2022) Carbon-black combined with TiO2 and KuQ as sustainable photosystem for a reliable self-powered photoelectrochemical biosensor. Electrochim Acta 426:140766. https://doi.org/10.1016/j.electacta.2022.140766
188. Liu Y, Ai S, Yuan R, Liu H (2022) Defective Se-doped In2S3 nanomaterial-based photoelectrochemical biosensor for the ultrasensitive detection of chloramphenicol. Sensors Actuators B Chem 373:132705. https://doi.org/10.1016/j.snb.2022.132705
189. Du H, Xue Y, Wang C, Jie G (2022) ZnIn2S4 QDs@TiO2 nanosphere-BiOI double heterojunction combined with unique tripod DNA walker amplification for photoelectrochemical biosensing of microRNA-21. Sensors Actuators B Chem 373:132704. https://doi.org/10.1016/j.snb.2022.132704
190. Zheng Y, Zhou Y, Cui X et al (2022) Enhanced photoactivity of CdS nanorods by MXene and ZnSnO3: application in photoelectrochemical biosensor for the effect of environmental pollutants on DNA hydroxymethylation in wheat tissues. Mater Today Chem 24:100878. https://doi.org/10.1016/j.mtchem.2022.100878
191. Liu S, Dong H, Jiang F et al (2022) Self-powered photoelectrochemical biosensor with inherent potential for charge carriers drive. Biosens Bioelectron 211:114361. https://doi.org/10.1016/j.bios.2022.114361
192. Shabbir SA, Imran A, Ashiq MGB et al (2021) Photoelectrochemical response of non-enzymatic glucose biosensing for graphene, carbon nanotubes and BiVO4 nanocomposites. J Mater Sci Mater Electron 32:17741–17751. https://doi.org/10.1007/s10854-021-06310-w
193. Yang W, Xu W, Wang Y et al (2020) Photoelectrochemical glucose biosensor based on the heterogeneous facets of nanocrystalline TiO2/Au/glucose oxidase films. ACS Appl Nano Mater 3:2723–2732. https://doi.org/10.1021/acsanm.0c00086
194. Scott A, Sakib S, Saha S et al (2022) A portable and smartphone-operated photoelectrochemical reader for point-of-care biosensing. Electrochim Acta 419:140347. https://doi.org/10.1016/j.electacta.2022.140347
195. Barnawi N, Allehyani S, Seoudi R (2022) Biosynthesis and characterization of gold nanoparticles and its application in eliminating nickel from water. J Mater Res Technol 17:537–545. https://doi.org/10.1016/j.jmrt.2021.12.013
196. Jabbar ZH, Graimed BH, Okab AA et al (2023) A review study summarizes the main characterization techniques of nano-composite photocatalysts and their applications in photodegradation of organic pollutants. Environ Nanotechnology, Monit Manag 19:100765. https://doi.org/10.1016/j.enmm.2022.100765
197. Ruzik L (2023) Microalgae with active biological metal-nanoparticles as a novel food. Biosynthesis, characterization and bioavailability investigation – review. Trends Food Sci Technol 139:104127. https://doi.org/10.1016/j.tifs.2023.104127